Observing ocean currents on the Scottish Continental Shelf using Wave Gliders

MSc thesis

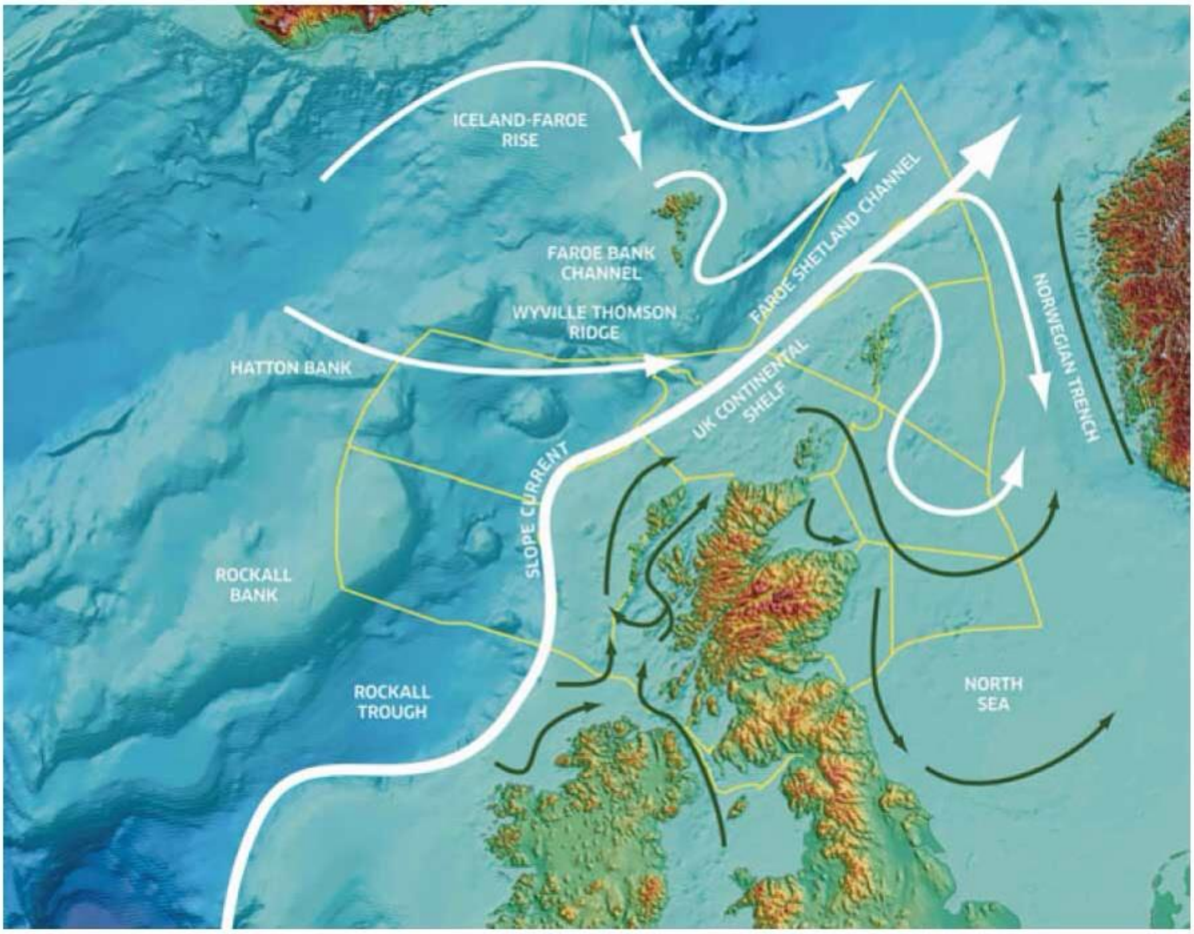

Siska de Vreeze
02-07-2020

marine scotland science

UNIVERSITY OF TWENTE.

Observing ocean currents on the Scottish Continental Shelf using Wave Gliders

MSc thesis

Author: Siska de Vreeze
Student number: s1647741
E-mail address: siska.v@hotmail.com

Master thesis

Educational program: Water Engineering and Management
Track: River and Coastal Engineering

Institution: University of Twente
Main supervisor: Prof. dr. Kathelijne Wijnberg
Daily supervisor: Johan Damveld, MSc
External supervisor: Dr. Bee Berx
External supervisor: Dr. Berit Rabe

Graduation period: February - July 2020
Aberdeen, July 2nd 2020

Preface

After 5 months of research, this thesis, "Observing ocean currents on the Scottish Continental Shelf using Wave Gliders", marks not only the end of my time at Marine Scotland Science, but also the end of my time as a student. It has not always been easy, but it has definitively been worth it. Therefore, I would like to thank my family first, because they have always supported me, and my friends, for the good stories and even better experiences we shared these past five years.

Of course, this thesis would not have existed without my supervisors. Therefore, I would like to thank all of them: Johan Damveld, my supervisor from the University of Twente, for helping me define my research objective, and for helping me tell the story I wanted to tell; my two supervisors at Marine Scotland, Bee Berx and Berit Rabe, for helping me understand the topic, for being patient with me when I did not yet understand certain oceanographic processes, and for making me feel at home in Aberdeen; Kathelijne Wijnberg, chair of my graduation committee, for guiding the process and making sure it came to a great end; and Bart Vermeulen, who was my first supervisor from the university, and helped to get me started. I would also like to thank all of them for their critical and very useful feedback.

Finally, I would like to thank the Oceanography group at Marine Scotland, who welcomed me with open arms. They made me feel welcome and at home in Aberdeen, even when Covid-19 prevented us from going into the office. I had a great time in Aberdeen, so thank you for having me. I will definitely come back to Scotland once the world goes back to normal.

I hope you will enjoy reading this thesis.

Siska de Vreeze
Aberdeen, July 2$^{\text{nd}}$, 2020

Summary

MASSMO (Marine Autonomous Systems in Support of Marine Observations) is a five-year research programme in UK waters using new Marine Autonomous Systems technologies (Wynn, 2019). As part of the third mission in this programme, MASSMO-3, in September 2016, three Wave Gliders were deployed northwest of Scotland. In this study, the quality of the data from these Wave Gliders is analysed, as well as the Wave Glider's ability to determine the tidal movements in an area and transport across a section. Furthermore, the circulation on the Scottish Continental Shelf (SCS) is investigated. Finally, transport variability along the main pathway of Atlantic water, from the edge of the UK Continental Shelf into the North Sea, is studied.

This study aims *to determine the applicability of Wave Gliders in observing and understanding oceanographic processes.*

The main research question is: "How can Wave Gliders be used to improve the understanding of oceanographic processes, using the Scottish Continental Shelf as a case study?" To guide the research, this research question is separated into three sub-questions:

1. What is the quality of the data retrieved from the Wave Gliders during the MASSMO-3 mission, when compared to historical and modelled data?

2. What is the variability of the circulation on the SCS in the region of the northern tip of the Western Isles?

3. How does the transport on the SCS and along its subsequent path into the North Sea vary?

First, the data quality was analysed by using the Root-Mean Square-Error (RMSE) and correlation as statistical methods. Then, a tidal analysis was performed, and finally, visual analyses of the residual currents, temperature and salinity were done, using data from a hydrodynamic model (AMM7). These analyses showed that the Wave Glider can reproduce the M2 tide with a 1-3 $cm\ s^{-1}$ error, when compared to a barotropic tidal model (Tidal Model Driver (TMD); (Egbert and Erofeeva, 2002)). This means an error of 6-15%. The correlation with the TMD is 0.98-0.99. The tidal analysis gave good results when the entire Wave Glider track was compared to the TMD, with a difference of 1-2 $cm\ s^{-1}$ for the major and minor axis of the tidal ellipses, 2° for the inclination, and 12° for the phase, which translates in a lag of approximately 25 minutes for the 12.42 hour M2 tidal cycle. Overall, the signs are that the Wave Glider is capable of measuring the tidal movement.

Second, to study the ability of the Wave Glider to determine the volume transport, one section of the Wave Glider track was selected. The velocity (determined by the ADCP on the Wave Glider and by a hydrodynamic model) across this section was multiplied by a respective area to calculate a transport. The transports are then integrated over the entire section. The results from this show that the Wave Glider gives a slightly lower transport rate than

AMM7 (0.95 Sv (1 Sv = 10^6 m^3 s^{-1}) and 1.1 Sv, respectively), but this is still within the variability of the AMM7 transport.

Third, the circulation on the SCS and the transport and variability on the main transport path of Atlantic Water from the shelf edge to the North Sea were determined. For this, the same procedure to calculate transport was used as before, except this time the transport was calculated for (predefined) sections on the shelf. For the variability of the circulation on the SCS, four sections were used: one from the tip of the Western Isles to the shelf edge (Shelf-4), one from the north-western tip of the Scottish coast to the shelf edge (Shelf-3), one from the southern tip of Orkney to the shelf edge (Shelf-2), and one between the Scottish mainland and the Western Isles (North Minch). It appeared that there is an increase in transport between Shelf-3 and Shelf-2 (0.75 Sv to 1.6 Sv), which could be connected to an Atlantic Inflow between those two sections from further offshore. Furthermore, the mean transport rate in November was lower than that of other months, this was caused by two meteorological events. Analyses of transport in November showed that wind conditions have a large impact on transport, especially on the Shelf sections. The temperature and salinity for these four sections were also investigated. Temperature-Salinity diagrams indicated that most of the shallower, close-to-the-coast stations carried water from the Scottish Continental Current. Deeper, more off-shore points also carried water from the North Atlantic Current.

The sections used for the calculation along the main transport path of the Atlantic water are the Ellet Line (from the southern tip of the Western Isles to the shelf edge), Shelf-4 (from the northern tip of the Western Isles to the shelf edge), Shelf-0 (from the southern tip of the Shetland Islands to the shelf edge), North Shetland (from the northern tip of the Shetland Islands northwards to the shelf edge), Fair Isle Gap (between the northern tip of Orkney and the southern tip of the Shetland Islands) and Feie-Shetland (between the northern tip of the Shetland Islands and the Norwegian coast). Analyses of these sections showed that the transport increases from the Ellet Line towards Shelf-0 (0.5 Sv to 3.2 Sv). All sections demonstrate approximately the same signals, and a cross-correlation analysis returned a lag of 0 days. This would mean that the signals are propagated within one day, which would be possible if the origin of these signals are meteorological events on the entire area. The lag between the Ellet Line and Feie-Shetland was calculated to be 4 days. However, Feie-Shetland is a complex section with also the Norwegian Coastal Current crossing it, which might mean that this lag is based on signals from different origins.

It can be concluded that Wave Gliders are suitable in determining tidal movements and transport. However, the spatial variability of the Wave Glider track should be kept to a minimum if possible, and deployment periods should ideally be long enough to determine more tidal constituents.

Contents

List of Figures

List of Tables

Chapter 1

Introduction

This chapter serves as an introduction to the thesis subject. First, the topic is clarified, then some theoretical context is given. After the research gap is determined, the research objective is explained, and research questions are described. Finally, the overall approach is discussed.

1.1 Research topic

MASSMO (Marine Autonomous Systems in Support of Marine Observations) is a five-year research programme in UK waters using new Marine Autonomous Systems technologies (Wynn, 2019). The programme uses surface vehicles and submarine gliders to take measurements and investigate characteristics of the Continental Shelf and the oceanographic processes that take place there (National Oceanography Centre). The first mission, MASSMO-1, in 2014, focussed on wildlife monitoring, and chlorophyll-a, temperature and salinity measurements. MASSMO-2 investigated Celtic Deep and its attractiveness to marine predators. The third mission in this programme, MASSMO-3, took place in September and October 2016. As part of the programme, three Wave Gliders were deployed on the Scottish Continental Shelf, northwest of Scotland, which is the study area of this research. MASSMO-4, in 2017, took place in the Faroe-Shetland Channel (FSC) and focussed on monitoring marine mammals and oceanographic features. In 2018, MASSMO-5 was used to determine how the Royal Navy can use Marine Autonomous Systems, with a focus on the outer shelf and the upper slope off northern Norway (National Oceanography Centre, 2018)

Due to mis-timing between the MASSMO-3 campaign and research vessel opportunities, no other oceanographic instrumentation was deployed to gather comparable measurements over the same time period. However, historical data and modelled data are available.

This thesis research focuses on oceanographic processes in the study area, and the Wave Glider's ability to observe these processes. Data from MASSMO-3 is analysed to determine the data quality of the Wave Gliders, and its ability to monitor oceanographic processes such as the tides. Furthermore, transport and circulation in the study area is investigated. Finally, the possible use of Wave Gliders in further studying these processes is described.

1.2 Theoretical context

1.2.1 Study area

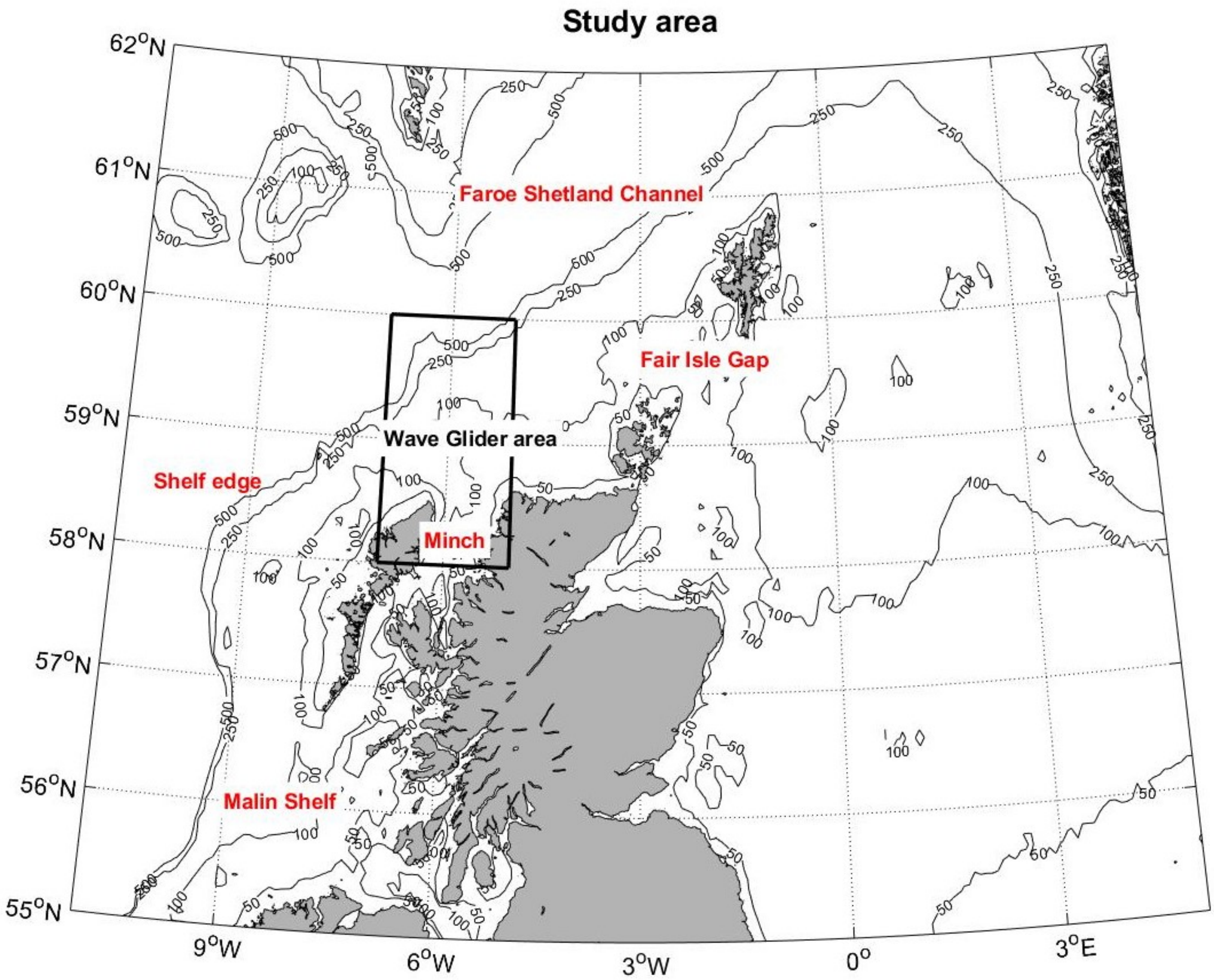

Figure 1.1: Study area, with in red some important areas. The area where the Wave Gliders were deployed, is shown in black.

This research is focused on the area north-west of Scotland, on the Scottish Continental Shelf (see Figure 1.1). This area is a shallow shelf region, with depths up to 200 metres at the shelf edge (Figure 1.2). Figure 1.2 also shows the movement of the tidal wave, northwards along the western edge of the shelf, then turning eastwards north of Scotland, and moving into the North Sea (Neill et al., 2017). The tides on the shelf are dominated by the semi-diurnal lunar (M2) and solar (S2) tides.

The non-tidal circulation in the study area is dominated by the Scottish Coastal Current (SCC; small green arrows near the Scottish coast in Figure 1.3) and the slope current (thick white arrow in Figure 1.3).

The SCC is a low salinity current carrying water from the Irish and Clyde Sea (Hill et al., 1997). A density gradient between the Irish Sea and the Malin Shelf (see Figure 1.1) moves

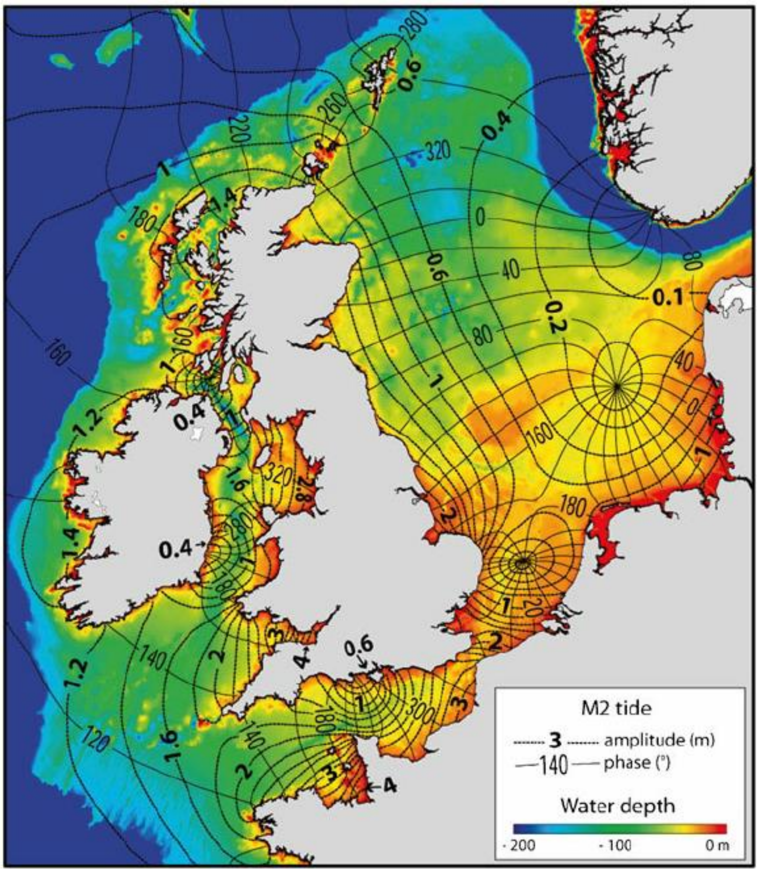

Figure 1.2: Amphidromic systems near Scotland. The colours represent the water depth, the shelf edge is shown in light blue. The lines represent the area that are either in the same phase, or have the same amplitude. The numbers represent the phase and amplitude. *Reprinted from: "Shallow-Marine Tidal Deposits", Reynaud Dalrymple, 2012, Principles of Tidal Sedimentology, p337*

the current northwards, although the near surface wind dominates the flow variability (Inall et al., 2009). Figure 1.4 shows a meander in the surface salinity isohalines in the Minch. This meander indicates a recirculation (Hill et al., 1997). The recirculation is clearly present during spring, visible during autumn, and not clearly present during summer. It might either mean that the current branches, after which one part travels further northwards through the Minch, and one goes around the outer islands, then north, or that some of the coastal water diffuses.

The slope current is topographically constrained along the continental shelf edge (the steep transition between the continental shelf and the deep Atlantic) (Porter et al., 2018). There is limited exchange between Atlantic water and coastal water (Jones et al., 2018). However, there are still some intrusions of Atlantic water. At about 55.5 °N, the Atlantic Inflow Current (AIC) joins the SCC. The variability in steepness and roughness of the slope influences the cross-slope exchange and slope current stability(Porter et al., 2018). The AIC at 55.5 °N may be the result of a destabilisation of the slope current, which could be caused by the change in slope direction (southwest-northeast to south-north), a change in slope gradient, and a deepening of the shelf break (Porter et al., 2018).

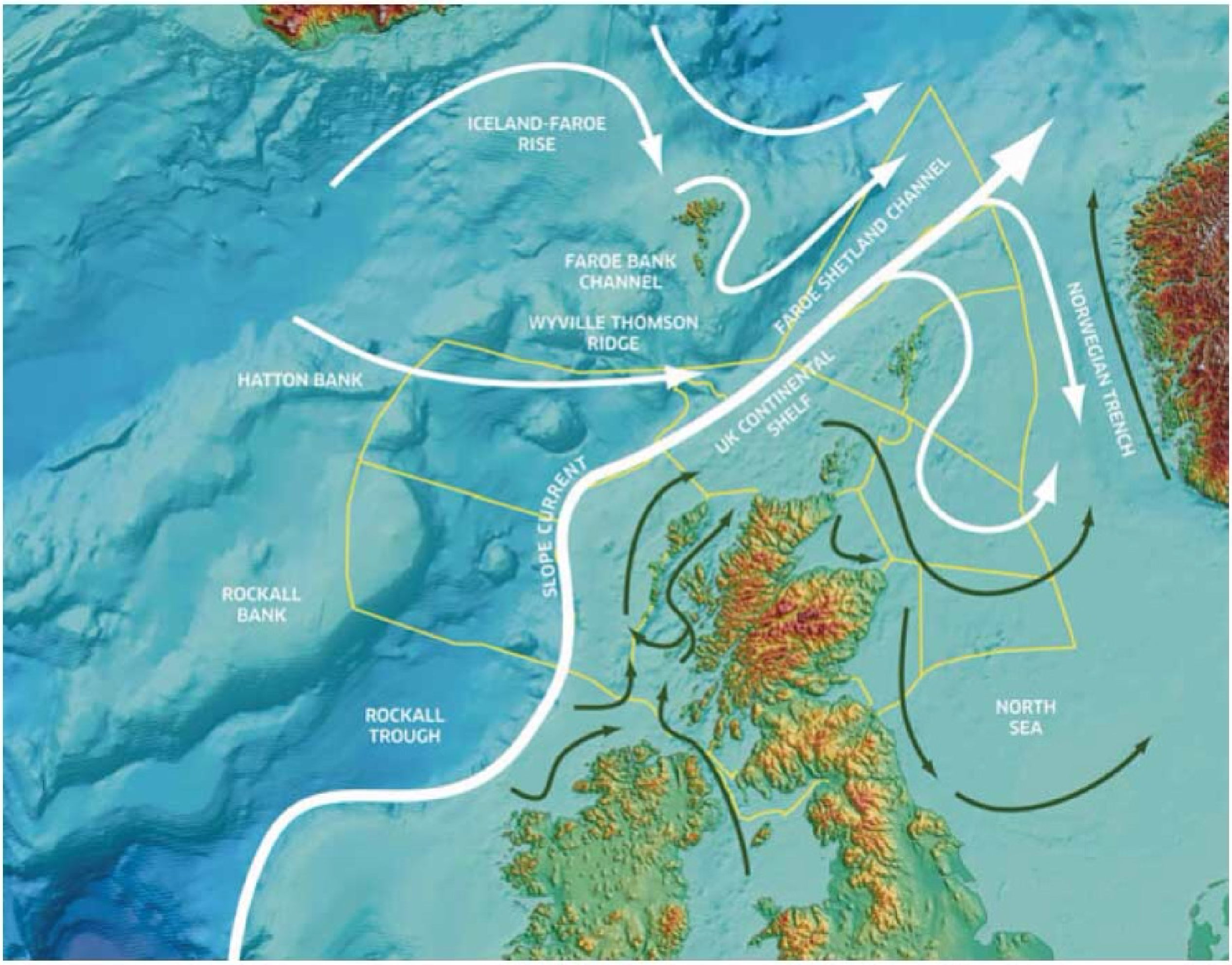

Figure 1.3: Circulation in the offshore and coastal waters around Scotland.The thick, white line along the shelf is the slope current. The white arrow just below the Wyville Thomson Ridge represents an Atlantic Inflow. The white arrows originating from the slope current, moving southwards, show how the Atlantic Water moves into the North Sea. Finally, the green arrows close to the Scottish coast, represent the Scottish Coastal Current. *Reprinted from: "Scotland's Marine Atlas", Baxter, J. M., Boyd, I. L., Cox, M., Donald, A. E., Malcolm, S. J., Miles, H., Miller, B., Moffat, C. F., (Editors), 2011, Marine Scotland, Edinburgh, p. 30*

1.2.2 Shelf transport

The currents described in the previous section, lead, together with other oceanographic processes and currents, to transport on the shelf.

Circulation and shelf transport have been increasingly investigated, especially with the development of drifters, CTDs, ADCPs and gliders (Holt and Proctor, 2008). Transport can be described as the simple transport of water through a section, or as the total transport of a water mass, where the water mass is identified by a certain salinity or temperature (Sherwin et al., 2008). Some of the water masses in the FSC are shown in Table 1.1 (Hansen and Østerhus, 2000).

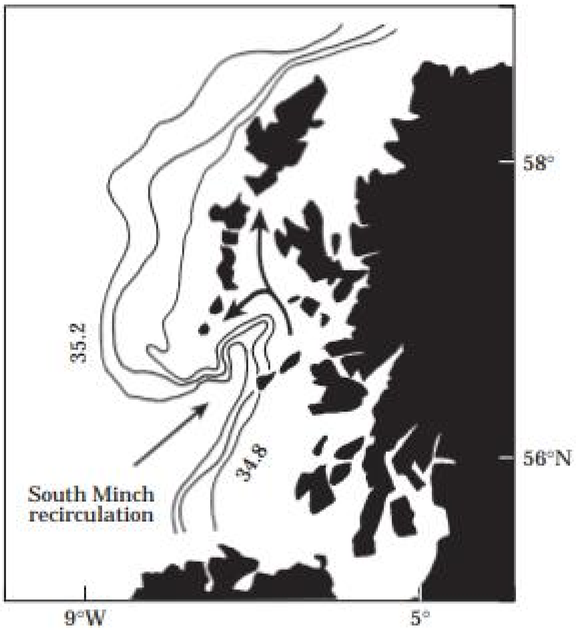

Figure 1.4: Surface salinity isohalines in the Minch. A clear meander is seen in the South Minch, where part of the current moves south of the Western Isles, then northwards along these Isles, and the other part flows through the Minch. The numbers represent the salinity, with fresher water closer to the coast, and more saline water further offshore. *Reprinted from: "Observations of a Density-driven Recirculation of the Scottish Coastal Current in the Minch", A. E. Hill, K. J. Horsburgh, R.W. Garvine, P. A. Gillibrand, G. Slesser, W. R. Turrell, and R. D. Adams, 1997, Estuarine, Coastal and Shelf Science (45), p. 474*

Acronym	**Name**	**Temperature [°C]**	**Salinity [-]**
MNAW	Modified North Atlantic Water	7.0 - 8.5	35.10 - 35.30
NAW	North Atlantic Water	9.5 - 10.5	35.35 - 35.45
MEIW	Modified East Icelandic Water	1.0 - 3.0	34.70 - 34.90
NSAIW	Norwegian Sea Arctic Intermediate Water	-0.5 - +0.5	34.87 - 34.90
NSDW	Norwegian Sea Deep Water	< -0.5	34.91

Table 1.1: Characteristics of water masses in the Faroe-Shetland Channel. Characteristic temperatures and salinities are shown. In the study area for this research, only North Atlantic Water (NAW) is expected.

Transport of water varies on different length and time scales (Sherwin et al., 2008). Variations take place on a millennial/centennial timescale, affecting the entire Atlantic Ocean or even the global circulation; on a decadal to inter-annual scale, affecting the North Atlantic Ocean; on a seasonal or monthly scale, influencing the regional scale; on a weekly timescale, influencing mesoscale motions; and lastly, as high frequency variations.

The seasonal timescale and shelf-wide space scale transport across the Northwest European Continental Shelf is investigated by Holt and Proctor (2008). They aimed to identify the relative importance of the wind-, density- and oceanic-driven circulation to this transport, and the importance of the effects of the bottom topography and friction, by using a hydrodynamic model with a fine spatial resolution, covering the entire shelf. They found that the wind-, density-, and oceanic forcing played an approximately equal role in the overall circulation pattern in the shelf seas. These results generally agree with Huthnance (1997), who states that there is a "strong external control" on the North Sea circulation. Holt and Proctor (2008) also show the importance of density-driven currents in the northern North Sea, during the break down of stratification, which takes place in late summer and autumn. However, they do not address the lateral mixing between coastal waters and Atlantic water, while this determines the overall exchange between coast and ocean.

Turrell et al. (1990) describe the residual transport within the Fair Isle Current (FIC), using observations from the Autumn Circulation Experiment (ACE). The ACE was a cooperation between five northern countries, running between September 1987 to January 1988. The experiment involved current meter moorings that were deployed at the same time along the coasts to the west of Scotland, to the north of Scotland and across the Northern Sea from Scotland to Norway. Turrell et al. (1990) analysed the transports to determine the driving mechanisms. They also used these observations from the ACE to study the FIC. The FIC is the inflow to the north of Orkney. It consists of a mixture of low salinity water from the west coast of Scotland and Atlantic water, and is generally vertically homogeneous. Possible driving mechanisms are the non-linear tidal interactions, wind stress, horizontal density gradients, and external oceanic forcing (Turrell et al., 1990). Generally, the residual volume transport in the FIC is assumed to result mostly from wind forcing. Observations of the FIC west of Orkney have shown that wind forcing causes the variability of the transport into the North Sea. Variations are also caused by the degree of stratification. Stratification is still present during September, October and November, when also a notable non-wind-driven component of the transport is observed. This component may be a result from the horizontal density gradients, resulting in baroclinic forcing. In December, the component is no longer present.

Sherwin et al. (2008) and Berx et al. (2013) looked into the transport through the FSC, which runs between the Faroe and Shetland Isles in the northern North-East Atlantic. According to Berx et al. (2013) two different water masses are found in the upper layers of the channel: North Atlantic Water (NAW) and Modified North Atlantic Water (MNAW). NAW is warmer and more saline water and is found over the west Shetland slope, flowing in a north-east direction. MNAW is found more in the centre and on the Faroese slope, flowing in a south-west direction. The density difference between the NAW and MNAW causes a strong front (Sherwin et al., 2008). Below these layers, at a depth of 400-600 metres, Arctic Intermediate Water (AIW) and Modified East Icelandic Water (MEIW) are found (Sherwin et al., 2008). Below 600 metres, Norwegian Sea Deep Water (NSDW) is flowing southward.

Sherwin et al. (2008) mention that observations suggest that the transport of NAW and MNAW is weakest in June and strongest in early winter. The monthly mean transport above 500 metres depth varies from 2.3 Sv (1 Sv = $10^6\ m^3\ s^{-1}$) in April to 4.1 Sv in August, with a standard deviation of 0.6 Sv. The minimum seems to be related with an increase in southward transport of MNAW. Tait (as cited in Sherwin et al. (2008)) used geostrophic calculations, and found values ranging between 0.4 to 6.5 Sv, and a mean value of 2.3 Sv. As this method of calculation does not cover the barotropic flow component, the mean value is underestimated. Sherwin et al. (2008) used ADCP derived estimates to get 3.2 Sv for the entire section, and 4.0 Sv for the NAW transport. Berx et al. (2013) combined ADCP, CTD and altimetry data from between 1995 and 2009, and estimate the Atlantic Water inflow through the FSC to be 2.7 Sv, with a standard deviation of 0.5 Sv. Contrary to Sherwin et al. (2008), Berx et al. (2013) find a maximum flow around the turn of the year. Furthermore, a seasonal amplitude of 0.7 Sv is found. Sherwin et al. (2008) state that approximately half of the north-east transport through the channel might be caused by the wind stress, and the rest by a north-south pressure gradient.

1.2.3 Wave Glider

Wave Gliders (Figure 1.5) are wave-and-solar powered autonomous surface vehicles, consisting of two main parts (Olson, 2012). A surface floater (float), with a length of approximately 2 metres, and a submerged glider (or sub) are connected with a flexible tether or umbilical (Wang et al., 2019a). Ocean wave motion is converted by the glider into a forward motion. A rudder on the glider ensures the Wave Glider stays on its pre-programmed course. The Wave Glider has an average speed of approximately 0.8 $m\ s^{-1}$, and can endure large open sea waves and strong winds (Wang et al., 2019a), powering through conditions as extreme as hurricanes (Liquid Robotics Inc., 2020b). However, the float and glider velocities oscillate with the wave motion, where the float velocity lags behind the glider velocity (Wang et al., 2019b). The required minimum depth for the Wave Glider depends on the length of the umbilical.

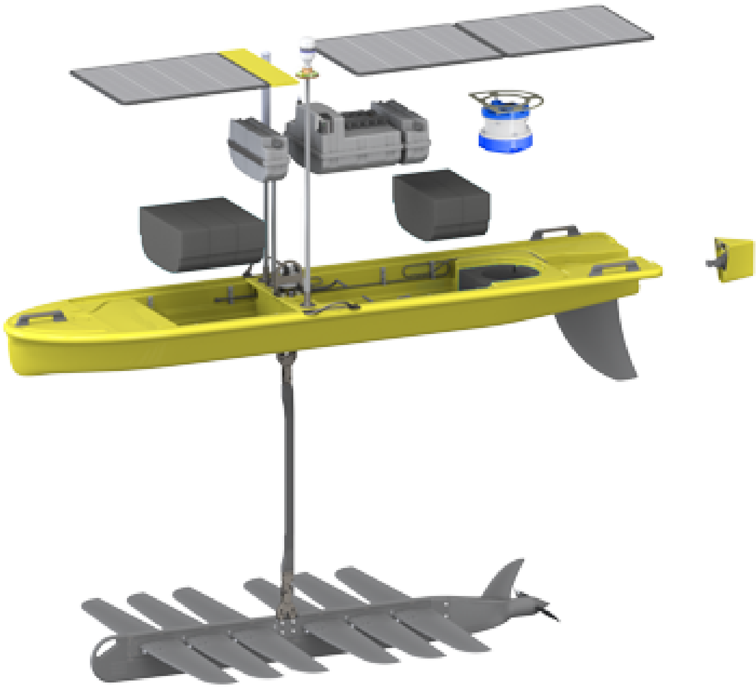

Figure 1.5: A deconstructed view of a Wave Glider, as used in this study, showing the solar panels, some instruments, the float, the umbilical and the glider. *Reprinted from: Liquid Robotics*

Since Wave Gliders are equipped with a solar panel and battery, they offer advantages in long-time and low-cost monitoring (Wang et al., 2019a);(Wang et al., 2019b) A large variety of sensors and instruments can be used, for example oxygen sensors, temperature, salinity, an ADCP, or even cameras. For this study, the most relevant sensors are the ADCP (Acoustic Doppler Current Profiler) and temperature, salinity and pressure sensors. Satellite communication components allow for onshore control (Wang et al., 2019a). Some possible applications of Wave Gliders are (Maritime Robotics AS., 2019):

- Environmental assessments
  - Meteorological and oceanographic measurements (used in this study)
  - Tsunami seismic monitoring
  - Fisheries stock management

- Maritime surveillance
  - Border protection
  - Illegal fishing
- Oil gas, other minerals
  - Hydrocarbon monitoring
  - Seismic survey
- Defence
  - Anti-submarine warfare
  - Surface vessel warfare

Wave Gliders have been successfully used in previous projects, such as:

- Japan's first long-term ocean observation network Liquid Robotics Inc. (2020a)
  The Japan Coast Guard used Wave Gliders to monitor the ocean environment of Japan more effectively. In the summer of 2016, Wave Gliders were employed in four regions to measure ocean currents, wave activity and weather. The data retrieved from the Wave Gliders is used to inform commercial and tourism industries of weather patterns and ocean conditions, to increase the safety and efficiency of their maritime operations.
- Monitoring marine protected areas Liquid Robotics Inc. (2020b)
  The UK Foreign and Commonwealth Office used a Wave Glider near the Pitcairn Islands to detect surface vessels in a remote marine habitat. This project had a duration of four months. The Wave Glider was controlled using satellite surveillance and expert knowledge of the area. The Wave Glider was equipped with a high-definition camera, which sent pictures of detected vessels to a command centre. Other sensors measured wind, pressure, temperature and sea-surface conditions. By using a Wave Glider instead of a manned vessel, the cost was reduced from 5.8 million dollars to a little over 200.000 dollars.

1.3 Research gap

While a lot about transport on the shelf is already known, a lot about the area north-west of Scotland is still unknown. Also, how Wave Gliders can contribute to understanding these processes further, is yet unknown. As described in de Vreeze (2020), Sheehan et al. (2018) performed a study involving ocean gliders in understanding tidal velocities. This study showed that ocean gliders can be used to observe and understand tidal velocities. However, the technology of ocean gliders is different from that of the Wave Gliders.
Therefore, the research gap that can be defined, consists of two sections: the characteristics and variation of transport on the shelf in the study area, and how Wave Gliders can be used to further study this and other oceanographic processes.

1.4 Research objective and research questions

Based on the knowledge gap described above, the following research objective will be investigated: *to determine the applicability of Wave Gliders in observing and understanding oceanographic processes.*

The research will focus on the study area as mentioned in section 1.2.1.. However, when looking for other applications of Wave Gliders, other locations may be taken into account as well. Furthermore, the only autonomous technology used in the research will be the Liquid Robotics Wave Glider. This is the type of autonomous technology that was used in the MASSMO3 project, and all observed data is measured by these Wave Gliders. The research objective is translated into the following main research question:

"How can wave gliders be used to improve the understanding of oceanographic processes, using the Scottish Continental Shelf as a case study?"

To guide the research, the research question is split into sub-questions:

1. What is the quality of the data retrieved from the Wave Gliders during the MASSMO-3 mission, when compared to historical and modelled data?
   This sub-question is answered using statistical methods (root-mean square-error and correlation), harmonic analyses, and a visual analysis.

2. What is the variability of the circulation on the Scottish Continental Shelf (SCS) in the region of the northern tip of the Western Isles?
   For this sub-question, the transport for several sections is calculated. Variability in these rates is explained using meteorological data. Finally, water masses are distinguished on the sections.

3. How does the transport on the SCS and along its subsequent path into the North Sea vary?
   This sub-question uses a similar approach to sub-question 2, but has a focus on the propagation of signals from section to section.

1.5 Overall approach

First, all data is collected: velocity magnitude and direction from the ADCP on one Wave Glider; the temperature and salinity data from all three Wave Gliders; temperature and current velocity data from three moorings; current velocities from a tidal model on 16 locations along the Wave Glider track and at the locations of the moorings; current velocity, temperature and salinity data from a hydrodynamic model; and surface air pressure, wind direction and wind speed data from a climate reanalysis.
Second, the data quality of the Wave Glider is determined. De-tided data is used to calculate the Root-Mean Square Error (RMSE) and correlation. The current velocities from the tidal model are compared to those of the moorings and the Wave Glider. Also, the influence of the spatial variability (the area covered by the Wave Glider) of the Wave Glider track on the data quality is determined. Finally, the tidal analysis of the Wave Glider data is compared to that of the tidal modal and the moorings.
Lastly, the transport across several sections is determined, using data from the hydrodynamic model. For this, the current velocity at several depth levels is multiplied by the area of its artificial grid cell. For the variability of the circulation, four sections in the region of the northern tip of the Western Isles are used. Monthly and weekly means are calculated, and the variations in this transport are analysed using the climate data. For the variation along the path of Atlantic Water from the edge of the shelf into the North Sea, the weekly mean transport across six sections on the shelf is determined. Then, the propagation of these signals are analysed.

1.6 Thesis outline

This thesis is organized as follows (Figure 1.6). The methodology is described in Chapter 2. The results are given in Chapter 3. In Chapter 4, these results are discussed, as well as the limitations and implications of this research. The conclusions can be found in Chapter 5. Finally, some recommendations are made in Chapter 6.

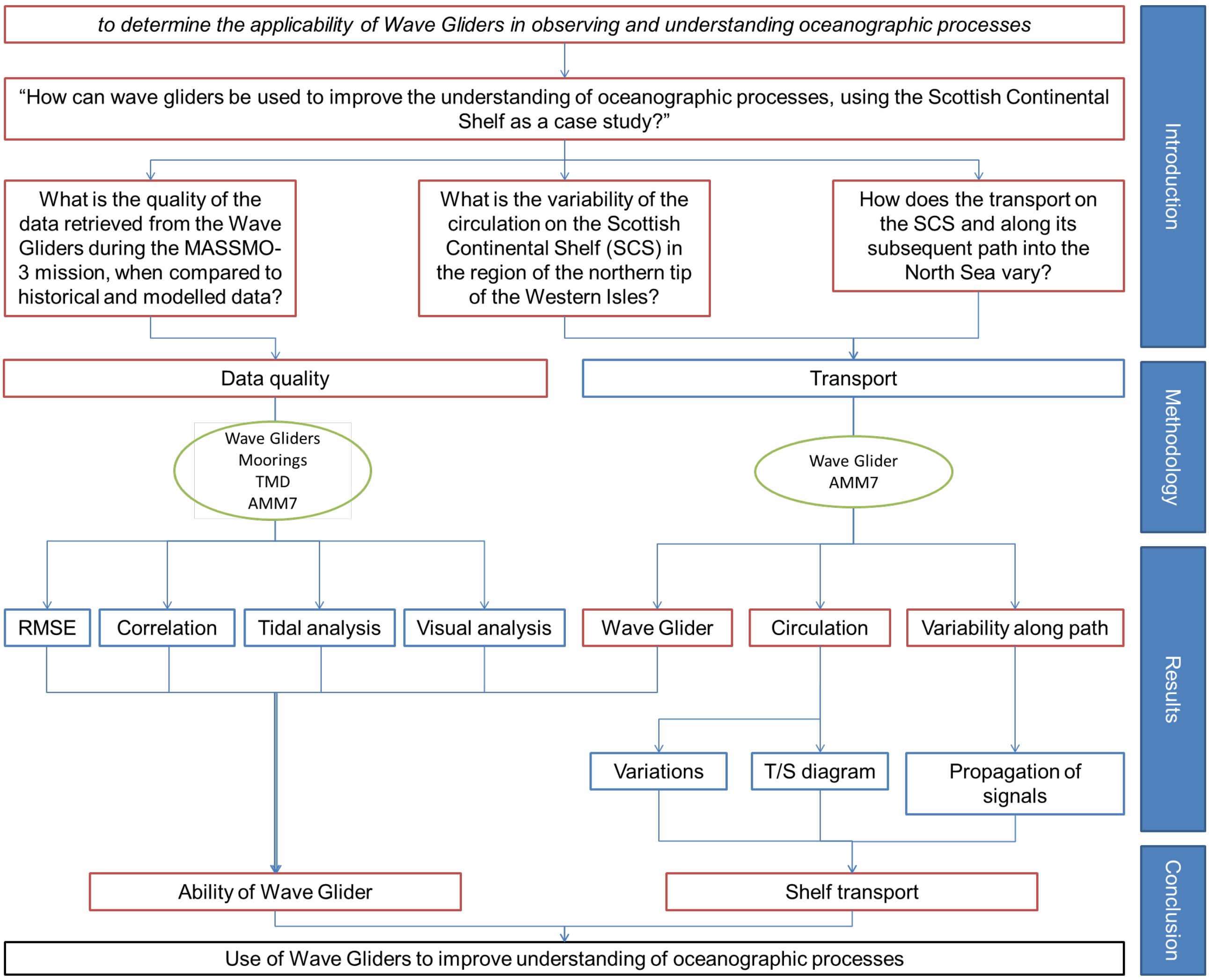

Figure 1.6: The outline of this thesis. The blue squares represent methods, the red squares are guiding the research. The green ovals represent data sets. The blue squares on the side are the chapters.

Chapter 2

Methodology

This chapter describes the methodology used to answer the sub-questions. The first, general, steps are explained, and then the methods for each question are given.

2.1 Data collection

To answer the main research question and sub-questions, a range of quantitative data is used. This quantitative data was sourced from several instruments and models for the study area: the three Wave Gliders used in the study area during MASSMO-3, three oceanographic moorings, the ES2008 model from the Tidal Model Driver, the AMM7 model, and climate data from the ERA5 reanalysis. These data sources are discussed in detail in the following section. Also, the criteria to select the data are described.

Wave Glider (s/n)	**Start date**	**End date**	**Glider depth [m]**	**Parameters measured**
26	19-09-2016 10:00	30-09-2016 10:24	8	Current velocities and direction Pressure Temperature Salinity Oxygen
117	19-09-2016 10:33	29-09-2016 16:33	8	Pressure Temperature Salinity Oxygen
127	19-09-2016 09:48	10-10-2016 10:04	20	Pressure Temperature Salinity Oxygen

Table 2.1: Wave Glider data. For each Wave Glider (characterised by serial number (s/n)), the start and end date, glider depth and measured parameters are presented.

2.1.1 Wave Glider data

Temperature, salinity, pressure and oxygen data, measured by a CTD, from all three Wave Gliders were retrieved from the British Oceanographic Data Centre. ADCP data from the Waimea Wave Glider (serial number (s/n) 26) was received from the National Oceanography Centre. The CTD was placed on the sub of each glider, which means that for the Waimea

Wave Glider, and one Boeing Wave Glider (s/n 117), the CTD measured at a depth of 8 metres below the sea surface. The sub of the other Boeing Wave Glider (s/n 127) was located at a depth of 20 metres below the sea surface. The measurements for all Wave Gliders were taken as burst measurements, with groups of measurements approximately 15 minutes apart. The ADCP was installed on the float of the Waimea Wave Glider. It measured the magnitude and direction of the currents at 25 depth bins, from 2.1 to 26.1 metres below the surface, with intervals of 1 metre. Five measurements were taken each hour, at approximately 2, 4, 6, 8 and 10 minutes past the hour. The Wave Glider tracks can be seen in Figure 2.1.

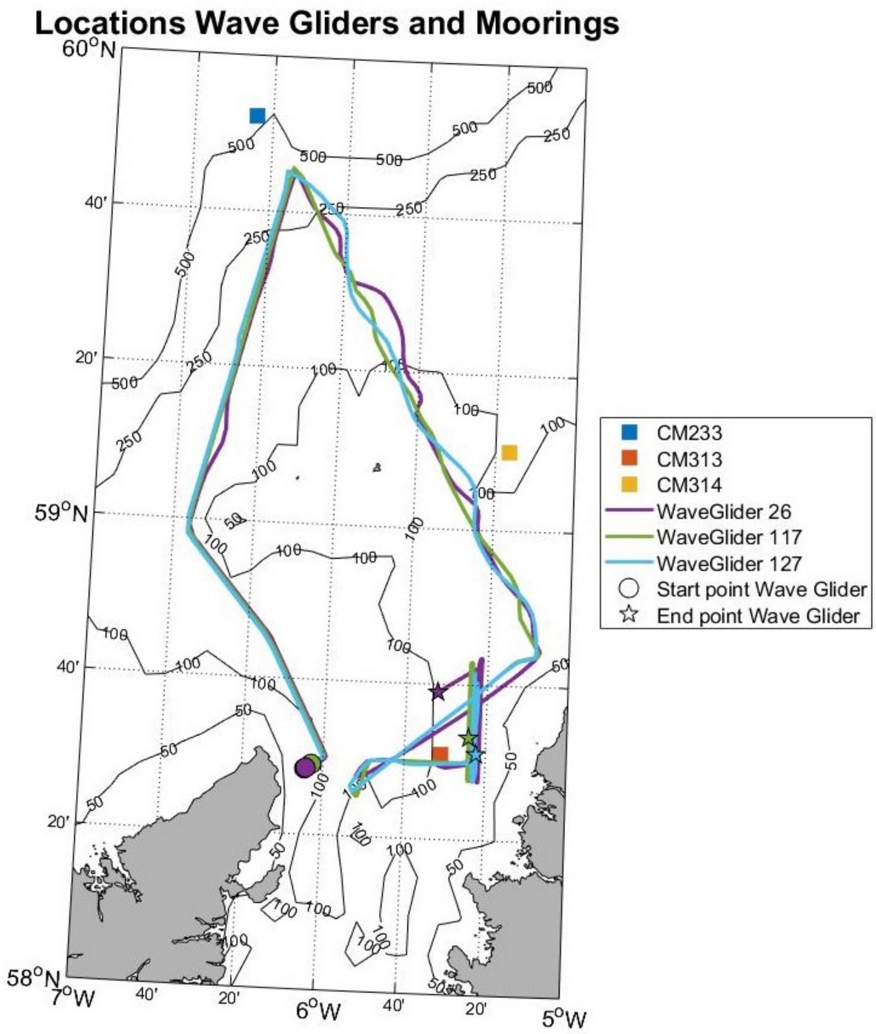

Figure 2.1: Overview of Wave Glider track and locations of moorings. Squares represent the moorings, lines represent the three Wave Gliders. The begin- and endpoints are represented by circles and stars, respectively. The figure also displays the topograhpy, which shows that the Wave Glider moves just onto the edge of the shelf.

2.1.2 Moorings

All three moorings, that were deployed within our study area, were equipped with Aanderaa instruments and measured current velocities and temperatures. The details on which mooring measured when and where, are shown in Table 2.2. The moorings use older instrumentation, this could cause some issues. The older instruments have a lower resolution, which could lead to less accurate measurements. However, there have not been any recent mooring deployments in this area at this time of year.

Mooring	**Start date**	**End date**	**Depth [m]**
CM233	01-06-1983	12-12-1983	100, 477
CM313	25-06-1989	26-09-1989	29, 104
CM314	26-06-1989	29-09-1989	40, 115

Table 2.2: Overview mooring data. The locations of the moorings can be seen in Figure 2.1. For each mooring, the start and end date, and depths are given.

2.1.3 TMD

The Tidal Model Driver is a Matlab package that can access tide models developed by Earth Space Research (ESR) and Oregon State University (OSU) (Erofeeva and Egbert, 2010). One of these models, used here, is the ES2008 model. This model was developed in 2008 for the European Shelf, with a resolution of 1/30°. It contains the M2, S2, N2, K2, K1, O1, P1, Q1, M4, MS4 and MN4 tidal constituents. The model can predict the tide with hourly values at certain locations. It can also give the tidal constituents for a location, either with the amplitude or with the tidal ellipses.

2.1.4 AMM7

The Atlantic Margin Model is a numerical model developed by the Met Office in collaboration with the NOC (Graham et al., 2018). The AMM models is an implementation of the Nucleus for European Modelling of the Ocean (NEMO) hydrodynamic model package (E.U. Copernicus Marine Service Information, 2018). AMM7 is the 7 km resolution model, a 1.5 km resolution model was introduced more recently (Graham et al., 2018). The AMM7 model assimilates observations of sea surface temperature and vertical temperature and salinity profiles. Vertically varying temperature, salinity and currents are interpolated to 24 standard depths, ranging from 0 to 5000 metres (National Oceanography Centre) (Tonani, 2019). The resolution in depth is highest near the surface, and decreases with depth. All datasets are monthly and daily de-tided averages.

2.1.5 ERA5

ERA5 is an atmospheric reanalysis developed by the European Centre for Medium-Range Weather Forecasts (ECMWF) (Copernicus, 2018). The reanalysis data is created by combining observations with a previous forecast, to form a new best estimate of the atmospheric state. The reanalysis resolution is 0.25° for the atmosphere, and data is given in hourly averages. The used datasets from ERA5 include the wind components and mean sea level pressure, as these might have an influence on the transports measured. The wind components (eastward (u) and northward (v)) are determined at 10 metres above the surface of the earth, and are measured in $m\ s^{-1}$. The mean sea level pressure is the force per unit area at the height of mean sea level, in Pascals (Pa).

2.2 Data selection

From all the data collected, a selection was made to limit the amount of data. First of all, only Wave Glider data with known units or conversion methods were used, as information about this data was scarce. For the moorings, one selection criteria was timing, data was required for the end of September to be able to be compared to the Wave Glider data. The moorings listed in Table 2.2 already meet this requirement. Furthermore, they had to measure in the vicinity of the Wave Glider track, so conditions would be similar. The TMD data locations were set to be at the same locations as the selected moorings, with 14 extra points at equal time intervals along the Wave Glider track. The time period was chosen to match the Wave Gliders measurements. For each location, a time series with just the M2 tide was retrieved, as it is expected that the local conditions are mostly guided by the M2 tide, and the time series length of the Wave Glider is too short to distinguish other tidal constituents. For the AMM7 data, the reanalyses for the current velocities, temperature and salinity for all of 2016 were used. The ERA5 data was selected for November. The spatial domain for both datasets was 55-62 °N and 5 °E -11 °W.

2.3 SQ1: Data quality

2.3.1 Data preparation

For all Wave Glider data, the data was first plotted and visually inspected to spot obvious errors, such as missing data or spikes. Also, the out-of-water data was removed from the data set. Then, the data was averaged into hourly values. For the ADCP data, this meant that the measurements at 2, 4, 6, 8 and 10 minutes past the hour were averaged. It is assumed that this average is representative for the whole hour. As the measurements became irregular at a certain point, the averaging method always took all points within a one hour window into account, no matter how many samples there were. The reason for the irregular measuring remains unclear, but might be connected to technical issues. For the CTD data, the same method was used, but for an interval of 15 minutes between measurements. For both the ADCP and CTD data, to construct a time series, the spatial variability (i.e., the area covered by the Wave Glider track) was not taken into account. Therefore, the Wave Glider data was considered to be measured at one location. Also, the ADCP data was depth-averaged for the first sub-question. The Wave Glider and TMD data sets were also split into three boxes (Figure 2.2), where the tidal ellipses are similar (based on a visual analysis), for ease of analysis. Tidal ellipses are plots of the tidal current vectors. During one tidal cycle, the current velocity vectors trace out this tidal ellipse shape (Thompson et al., 2005). The boxes were determined using the tidal ellipses from POLPRED. POLPRED is an offshore tidal software developed by the NOC.

For the Wave Glider data, the division into boxes means that each box contains only the part of the time series that the Wave Glider spent in that area. So, for example for Box 2, the time series starts when the Wave Glider travels into the box, ends when it leaves the box and moves on to Box 3, starts again when it moves from Box 3 to Box 2, and then finally ends when the Wave Glider again reaches Box 1.
When the boxes were determined, the moorings and model points were assigned to the box they were closest to.

The splitting of the Wave Glider data resulted in two discontinuous time series, and one continuous time series for the top box. A fourth box was added (Figure 2.2), in the southeast

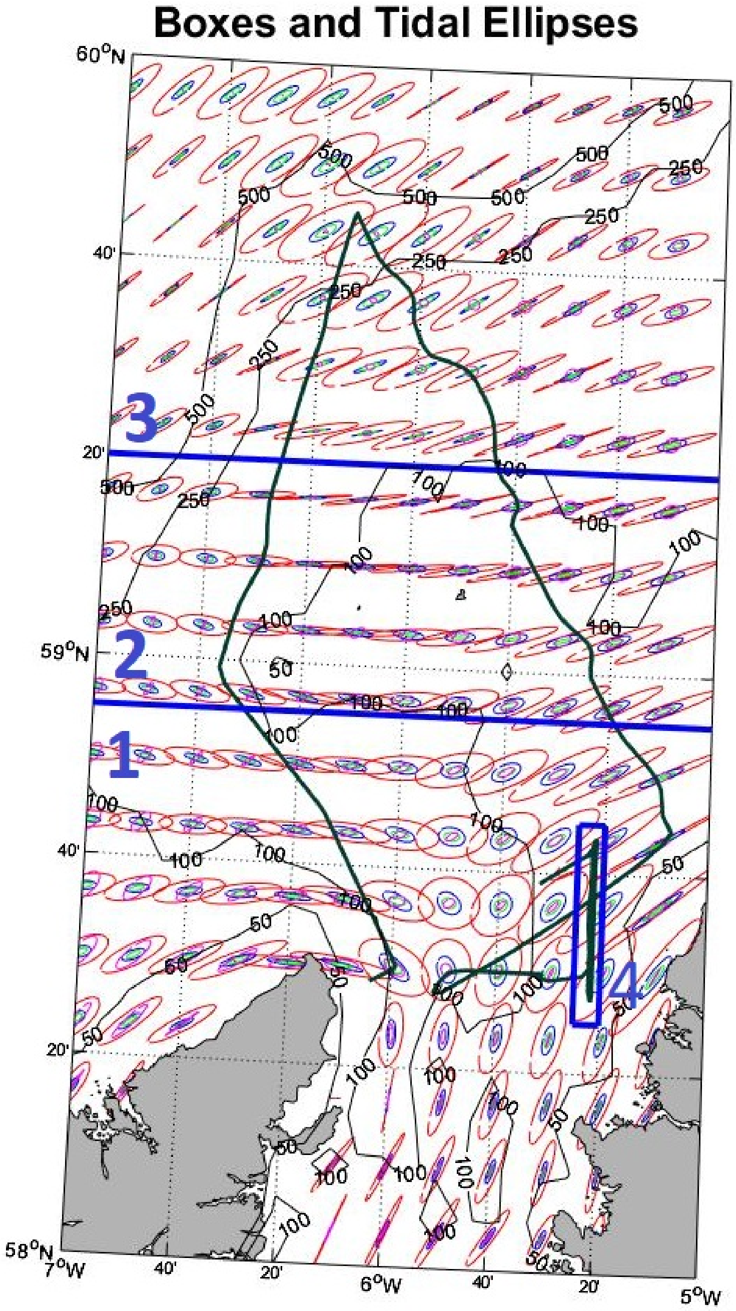

Figure 2.2: Tidal ellipses (based on the POLPRED data set) in study area, as well as locations of the boxes. The blue lines represent the separation between the boxes. The numbers indicate the box number. The red ovals are the ellipses for the M2 tidal constituent, the blue ovals represent the S2 constituents. The Wave Glider track is shown as a dark line.

corner of the Wave Glider track, as the Wave Gliders remained in this area for a few days. A mooring (and therefore a model point) was located in this box as well.

Finally, the current velocities were de-tided, by running the t_tide (Pawlowicz et al., 2002) module from Matlab, and subtracting the resulting predicted tide from each time series.

For the moorings, data from CM313 and CM314 had to be converted to hourly averages, as these moorings measured every half hour. For this, pairs of measurements on the hour and on the half hour are averaged. Then, all data was de-tided, following the procedure detailed above.

As the data from the TMD is already given in hourly values, the only preparation was the selection of the time period, the same period as the Wave Glider data was chosen.

For the AMM7 data, the only preparation required was the conversion from ms^{-1} to cms^{-1} for the current velocities.

2.3.2 Statistical methods

The statistical methods used to determine the quality of the Wave Glider data are the Root Mean Square Error (RMSE), correlation, a tidal analysis using t_tide in Matlab, and a harmonic analysis. First, the t_tide function was used on all time series. This resulted in values for the M2 tidal constituent, which were then used to predict a tide for September 19$^{\text{th}}$ to September 30$^{\text{th}}$, corresponding with the Wave Glider deployment period. Then, the TMD current velocities were compared to the predicted tides for the moorings and the Wave Glider, using the RMSE and correlation methods. For the moorings, the RMSE and correlation for the TMD data with regard to each mooring is determined. For the Wave glider, an average of fourteen model points is considered for the entire time series. For the boxes, the model points in the boxes are averaged. In Matlab, the RMSE was calculated as follows:

$$RMSE_{mooring} = rms(Mooring - Model) \tag{2.1}$$

$$RMSE_{WaveGlider} = rms(WaveGlider - Model) \tag{2.2}$$

The rms function calculates the following:

$$rms = \sqrt{\frac{\sum_{i=1}^{N}(x_i - y_i)^2}{N}} \tag{2.3}$$

N is the number of data points, x is either the mooring or Wave Glider data, and y is the TMD data. The calculation of correlation looks as follows in Matlab:

$$corr = corr(Model, Mooring) \tag{2.4}$$

$$corr = corr(Model, WaveGlider) \tag{2.5}$$

This corresponds to the following calculation:

$$corr = \frac{1}{N-1}\frac{\sum_{i=1}^{N}(x_i - \bar{x})\sum_{i=1}^{N}(y_i - \bar{y})}{s_x s_y} \tag{2.6}$$

Here, N is the number of observations. $\bar{x}$ and $\bar{y}$ are the mean values of each time series and s_x and s_y are the standard deviations of each time series.

Tidal analyses were performed on the Wave Glider ADCP data, the moorings data, and the TMD data. A tidal analysis on the tidal ellipses (using the complex number u+iv) was performed. This was done for the complete time series, and averages of the moorings and the TMD model. The tidal analysis was performed using the results of the t_tide function. This calculates the amplitudes or tidal ellipses for a number of tidal constituents, depending on the length of the time series, which has an influence on the distinguishable tidal constituents.

Emery and Thomson (2001) explain the required time series length required to solve for certain constituents. Some main tidal constituents are given in Table 2.3. The frequency for the tidal constituents is given in cycles-per-hour.

Tidal constituent	**Frequency [cph]**	**Required record length [h]**
M2 (principal lunar)	0.0805	13
S2 (principal solar)	0.0833	355
N2 (larger lunar elliptic)	0.0790	662
K2 (luni-solar)	0.0836	4383
K1 (luni-solar)	0.0418	24
O1 (principal lunar)	0.0387	328
P1 (principal solar)	0.0416	4383
Q1	0.0372	662
M_{sf} (mixed solar fortnightly)	0.002822	355
M_f (lunar fortnightly)	0.003050	4383
M_m (lunar monthly)	0.001512	764
M_{sm} (solar monthly)	0.001310	4942
S_{sa} (solar semi-annual)	0.000228	4383
S_a (solar annual)	0.000114	8766

Table 2.3: Names, frequencies and required record length for several tidal constituents. Frequency is given in cycles-per-hour, and required record length in hours.

As the Wave Glider time series is about 261 hours, the tidal analysis can be solved only for the M2 and K1 constituents. The t_tide module includes more tidal constituents than those in Table 2.3, so there some more tidal constituents can be discovered in the data. However, as the M2 and S2 tides have the greatest influence on the study area, other tidal constituents are ignored. The M2 tidal constituent was then compared for amplitude, phase, major and minor axis.

Furthermore, a harmonic analysis was performed on the Wave Glider data in each box. For this, a tidal constituent with a period of 12.5 hours was chosen. This period approximates the M2 tidal constituent. The results of this harmonic analysis consist of an amplitude and phase for the 12.5 hour period; a fitted data series (a sine with a 12.5 hour period, with the amplitude and phase determined from the time series); a residual of the fitted data series (i.e. the original time-series minus the fitted time series); and the r-squared (a measure of the amount of variance explained by the tidal constituent). To compare the Wave Glider data to the mooring and TMD data, the r-squared and amplitude are compared, in the same way as was done in the tidal analysis.

Finally, a visual analysis was performed, to compare the Wave Glider data with the AMM7 data. A quantitative analysis would have been possible, by extracting the temperature and salinity from the AMM7 data set for each data point of the Wave Glider time series. However, in this study, a visual analysis was chosen to limit the computation time.
Current velocities and directions were compared, as well as temperature and salinity. For Wave Gliders 26, 117 and 127 (differences between the values at 8 metres depth and 20 metres depth were very small), the measurements were averaged, as these both measured at the same depth, at roughly the same time. They were compared to the AMM7 data at a depth of 10m.

2.4 Volume transport calculation

To answer the second and third sub-question, the parameters u (eastward velocity), v (northward velocity), theta (temperature) and s (salinity) were extracted from the AMM7 dataset. Then, several sections were defined (Figure 2.3):

- For sub-question 2:
  - One section on the Wave Glider track, from the most northern point back towards the Scottish coast
  - Four sections in the wider vicinity of the study area (Shelf-4, North Minch, Shelf-3 and Shelf-2)
- For sub-question 3:
  - Six sections across the main transport path of the Atlantic water into the North Sea (Ellet Line, Shelf-4, Shelf-0, Fair Isle Gap, North Shetland and Feie-Shetland)

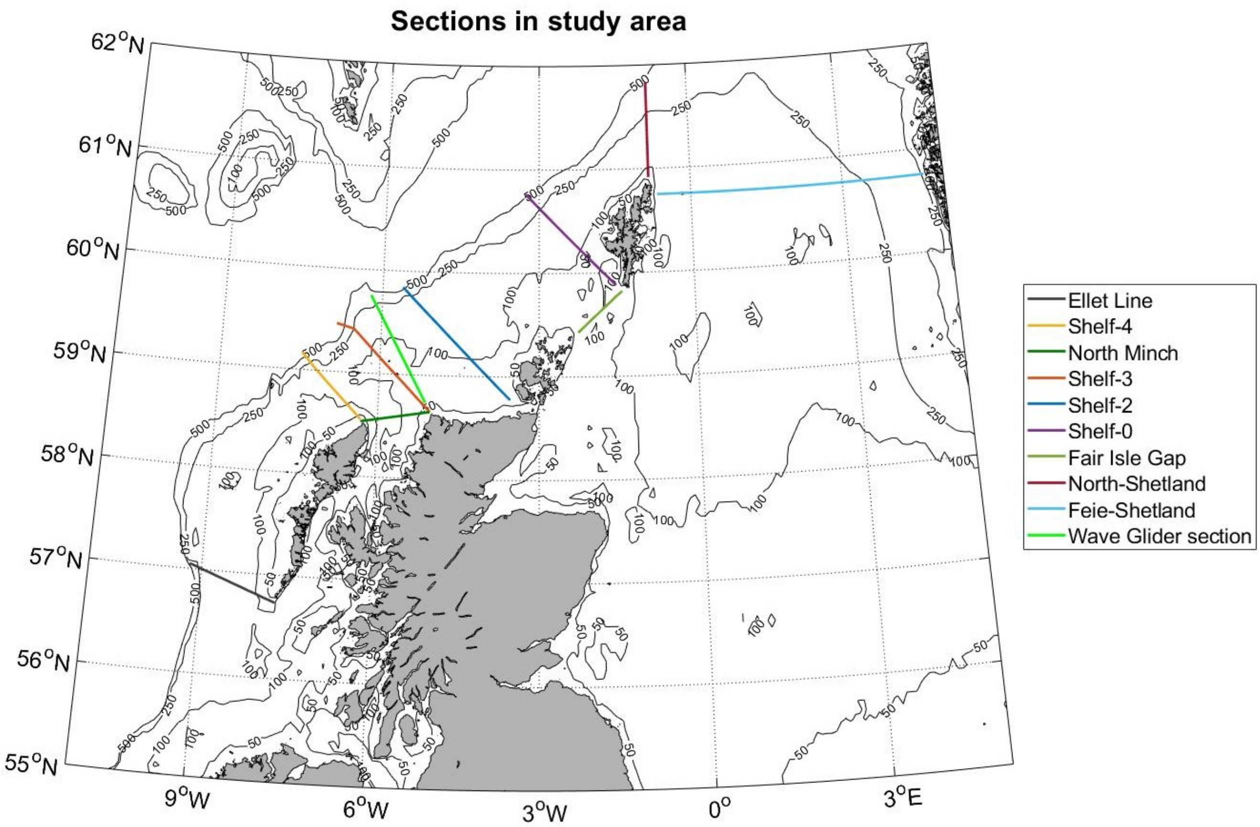

Figure 2.3: Defined sections for sub-questions 2 and 3. All sections are predefined, except for the North-Minch section and the Wave Glider section. The predefined Ellet Line is adapted to simplify calculations. All sections extend to the shelf edge, with the exception of the North-Minch, Fair Isle Gap, and Feie-Shetland sections, as these are connections between two coasts.

For each section, sampling stations were defined. The u, v, theta and s parameters were linearly interpolated onto these stations. The sections are located on the shelf, where water depths do not exceed 500 m. Therefore, for the interpolation, depths until 750 metres were used. The extra depth was used to ensure that all points were covered, should there be an outlier in depth. This interpolation resulted in daily values on the sections.

Next, the bearing between the start and endpoint of each section was calculated (Igis Map, 2020), which was then used to rotate the velocity to be perpendicular to the section. First, u and v are used to calculate the resultant velocity (U) (Figure 2.4) . Then, this velocity was broken down into two components; one parallel to the section (u'), and one perpendicular to the section (v'). Then, for the calculations, only the velocity (v') perpendicular to the section was used to calculate the transport. This velocity was defined as positive when it followed the main transport path, which for most sections is from southwest to northeast.

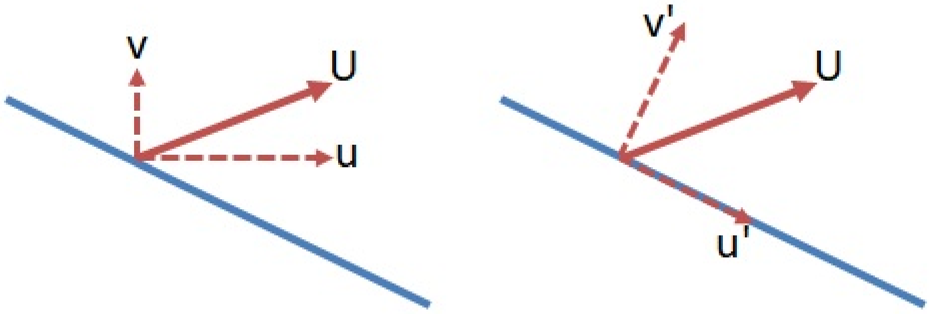

Figure 2.4: Explanation of the rotation. The red arrows represent velocities, the blue line represents a section. u and v components are used to calculate U, which is then decomposed into an along-section component (u'), and a cross-section component (v'). v' is then used to calculate the transport

To calculate the transport from the velocities, the cross-sectional area in the vertical is needed as well. To calculate this, first, the distance between the stations is calculated using the coordinates of each station (Williams, 2020). Figure 2.5 shows how the width and depth are determined for each station. For the begin- and end stations, the distance to the next (w_A) or previous (w_C) station is used. For the points in between, the sum of half the distance to the neighbouring stations (w_{Ba} and w_{Bb}, result in w_B) is used. The depth is determined in a similar way, with the exception being the point at the surface (Figure 2.5). This point has a depth of half the distance to the next point (d_{A1}). The width and depth are multiplied to get the area.
The transport for each grid point is calculated as the velocity times the area. These values were then divided by 10^6, to convert to Sverdrup (Sv). Finally, to get the (daily) transport values across the entire section, all values are summed up.

2.5 SQ2: Circulation

The first step in answering the second sub-question is to study the ability of the Wave Glider to determine transport across a section. As described in section 2.4, one part of the Wave Glider track was used for this. 12 sampling stations on this section were defined, all 10 kilometres apart. For the Wave Glider data, the highest spatial resolution possible would be 2 kilometres. Therefore, a smaller distance could be chosen, but this would result in a much longer computation time.

For the AMM7 data, the method as described in section 2.4 was used. The calculation for the Wave Glider data was very similar to this, with a few changes:

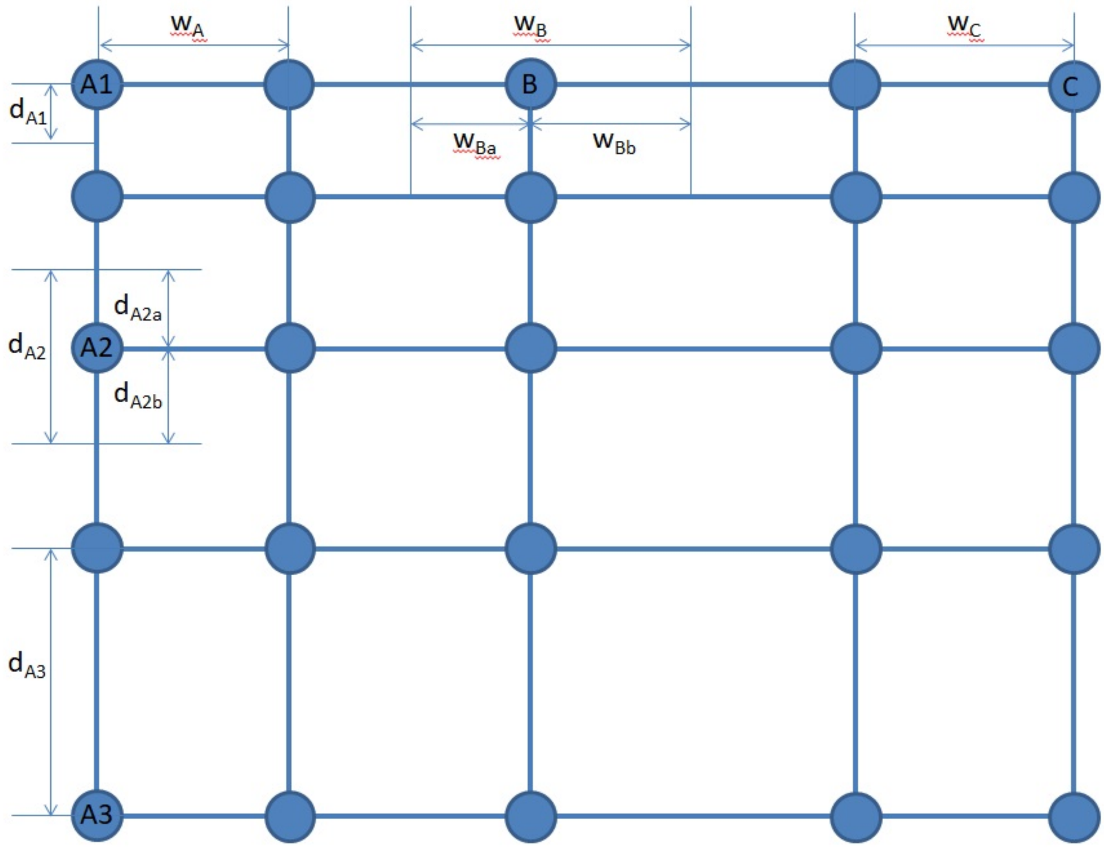

Figure 2.5: Determination of representative area for each station, a vertical cross-sectional schematisation of a section. Circles represent stations. A, B, and C are the horizontal locations for the stations; A1, A2 and A3 represent depth stations. The interval between depth stations increases toward the bed.

- First of all, the temporal aspect of the Wave Glider data was neglected, assuming that all measurements took place at the same time. In reality, the time difference between the first measurement on the section and the last was just over three days.
- Second, it was assumed that the velocity at 26 metres depth would remain constant to the seabed.
- Third, the distance between measurements was inconsistent, varying from only a few metres to 2 kilometres. The function griddedInterpolant, which was used for the AMM7 calculations, only works when these distances are constant. Therefore, it was assumed that these distances were constant.
- Fourth, the AMM7 gave daily values, whereas the Wave Glider gave one single value, as the temporal variability was neglected. Therefore, also the mean of the AMM7 was calculated for the month September, as well as the variability in this month.

Otherwise, the calculation for the Wave Glider data was the same as described in section 2.4.

To study circulation on the shelf, four sections in the wider vicinity of the study area were chosen (Figure 2.3): (from south to north) Shelf-4, North Minch, Shelf-3, and Shelf-2. Shelf-4, Shelf-3 and Shelf-2 are predefined, established sections in oceanographic research. The North Minch section was newly defined, this section crosses part of the Wave Glider track. It starts at the south-eastern most point of Shelf-4, and ends at the Scottish coast. Each section has sampling stations, several respectively 8, 15, 9 and 12 for Shelf-4, North Minch, Shelf-3 and Shelf-2. The predefined sections also included predefined stations. For Shelf-3, the station furthest away from the coast was removed, as this has a different bearing than the other stations. For the North Minch section, stations were defined every five kilometres.

Daily transport values showed large variability and therefore weekly (k-3 : k+3) and monthly (k-15 : k+15) running means were calculated. The weekly and monthly variability for these periods was also calculated, as well as the annual mean and annual variability.

To be able to identify specific water masses, T-S (Temperature-Salinity) diagrams are created. Temperatures and salinities for each section are averaged to create monthly means. These values are then distinguished by depth, month and distance to the coast, to create three T/S diagrams. Values for MNAW, NAW and the Scottish Coastal Current are also included in the figures. Finally, the temperature and salinity values for the Wave Gliders are added to the figures.

2.6 SQ3: Transport on the main path of Atlantic Water from the shelf edge to the North Sea

The first steps to answer research question 3 are similar as described in section 2.4. The following sections were used (Figure 2.3): the Ellet Line, Shelf-4, Shelf-0, the Fair Isle Gap, North Shetland and Feie-Shetland . All of these sections are predefined, established sections in oceanographic research. However, the Ellet Line is originally not a straight line across the shelf, and extends to Iceland. Therefore, this section was defined using the station south of the Western Isles, and a station at approximately the same depth as the most offshore station in section Shelf-4. Stations were then defined on the straight line connecting these two stations, with a distance of 5 km between them.

For the North Shetland and Feie-Shetland sections, the rotation step was unnecessary, as these are oriented northwards and eastwards, respectively. Therefore, for these sections, just the eastward and northward velocities were used, respectively.

From the daily values, the running weekly mean and variability were calculated. For most sections, transport was defined as positive when it moved from southwest to northeast. However, transport through the Fair Isle Gap moves from the northwest to southeast, when following the main transport path. Therefore, positive transport was defined as northwest to southeast.

To investigate the propagation of the variability signals (clear increases or decreases in transport that appear in all or most sections) between the sections, the weekly transport is standardized. This was done by removing the mean for each time series, and dividing the time series by the standard deviation. Then, a cross-correlation analysis was performed to determine the lags of the signals between the sections. In Matlab, cross-correlation is calculated by xcorr.

Chapter 3

Results

The results following the research are given in this chapter. They are also briefly discussed. An in-depth discussion and interpretation of the results can be found in Chapter 4.

3.1 SQ1: Data quality

To determine the quality of the Wave Glider data, the data was first visually checked for obvious errors or spikes and missing data, both by plotting the data and by calculating correlations between the three Wave Gliders and between the ADCP bins. The issues found were the following:

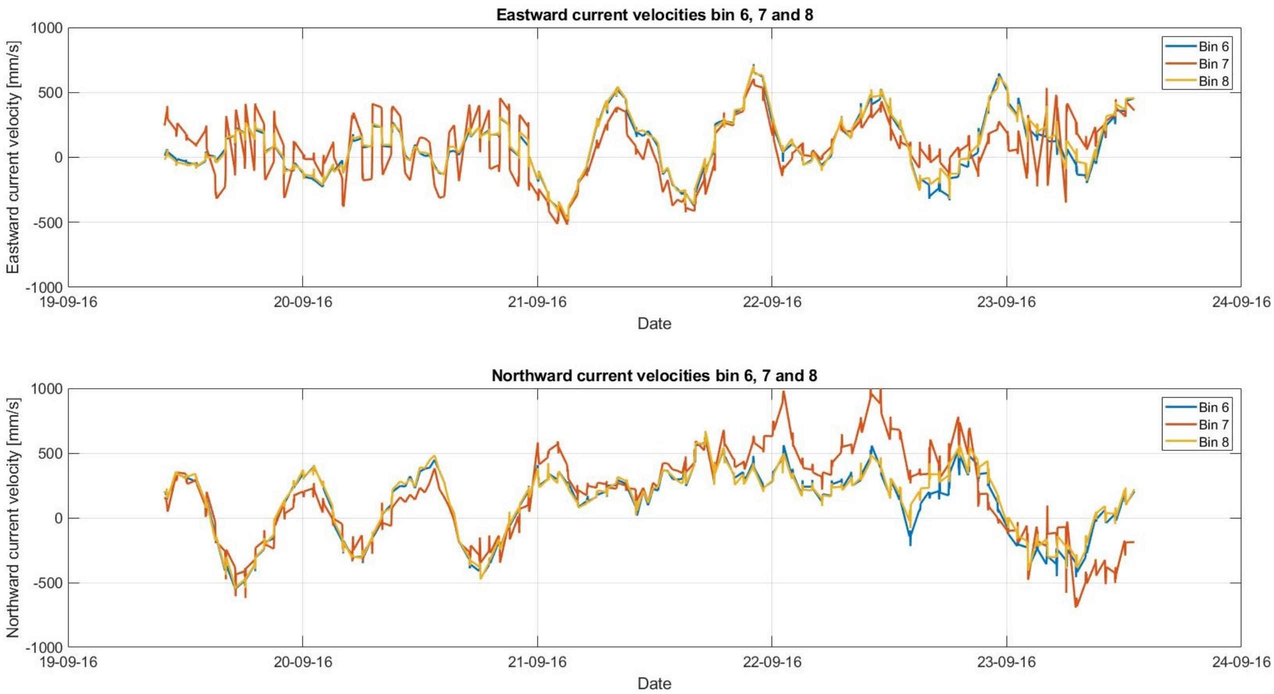

Figure 3.1: Current velocities for bin 6, 7 and 8, during the first four days of the Wave Glider deployment. Bin 7 shows clear deviations from bin 6 and 8, with values sometimes being twice as high (v-velocity, September 22$^{\text{nd}}$)

- For the ADCP data, bin 7 (at 8.1 metres), showed much more variability than the other 24 bins, which all gave approximately the same values (See Figure 3.1 for an example.

See Appendix A.1 for entire time series). This is especially obvious for the eastward velocity on September 20th, and for the northward velocity on September 22nd. The sub is located at 8 metres depth, and it is speculated that it might interfere with the ADCP signal. Therefore, bin 7 is recalculated as the average of bin 6 and bin 8.

- Wave Gliders 117 and 127 both had one day of data missing. For Wave Glider 117, no data was measured on September 27th, and Wave Glider 127 malfunctioned on September 28th. The reason for this malfunction remains unclear, but is likely connected to technical difficulties or a decision to reduce battery consumption. Data collection resumed as normal after those days.

Aside from these two issues, the Wave Gliders returned complete datasets.

3.1.1 RMSE

The first statistical method to determine the data quality of the Wave Gliders is the RMSE. Comparisons were made using predicted M2 tides for September 19th to September 30th 2016, for the TMD, moorings and Wave Glider ADCP data. The predicted tides for the TMD (only M2 tide) and Wave Glider data from September 22nd to 24th are shown in Figure 3.2. This figure shows that the predicted tides for both are similar, although the TMD lags slightly behind the Wave Glider. The other days are comparable to this period. The predicted tides for the entire time series and for the moorings can be seen in Appendix B.

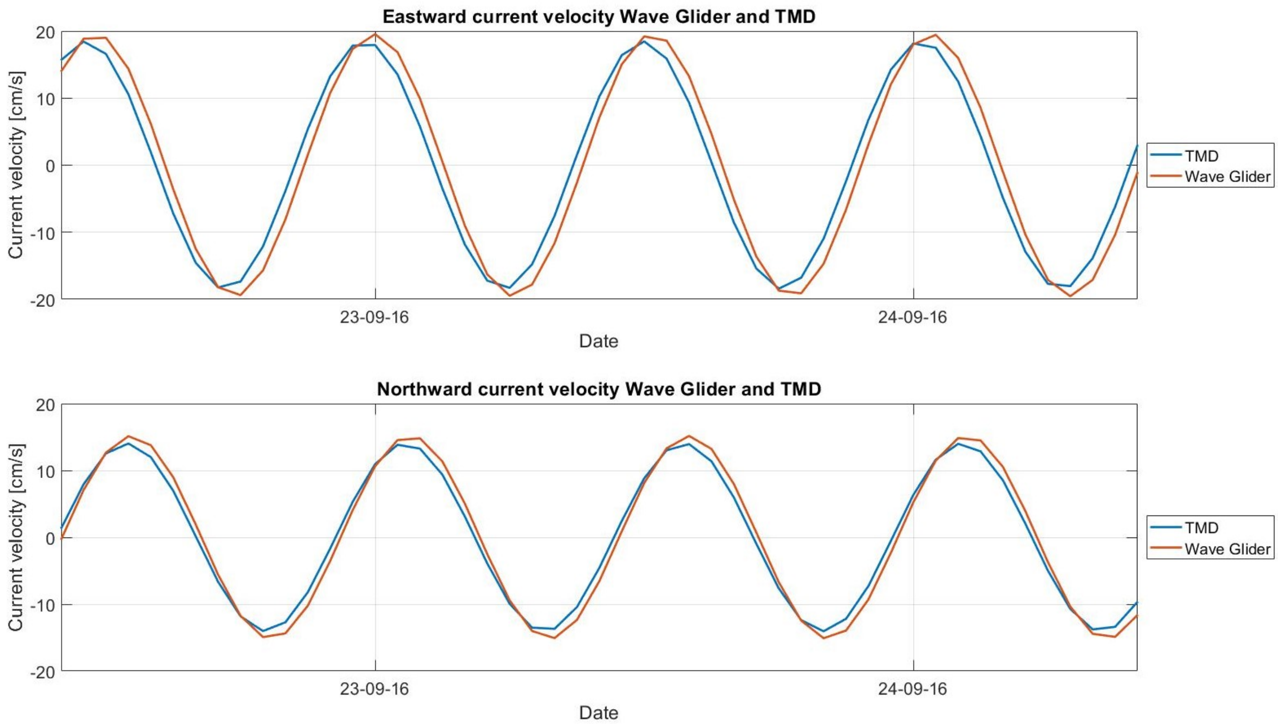

Figure 3.2: Predicted tide TMD and Wave Glider in $cm\ s^{-1}$. The TMD time series shows a slight lag with respect to the Wave Glider time series, but the amplitude is similar.

The RMSE results are shown in Table 3.1. The comparison between the TMD data and the Wave Glider data gives low RMSE values of 1-3 $cm\ s^{-1}$ when looking at the entire Wave Glider track. This value increases when only the boxes are compared. To provide some context: the predicted eastward velocity has an amplitude of approximately 19 $cm\ s^{-1}$, same as for example the RMSE of the v-component in Box 3; the predicted northward velocity has an amplitude of approximately 15 $cm\ s^{-1}$. The RMSE between the TMD and moorings data varies between 4-9 $cm\ s^{-1}$.

	u [$cm\ s^{-1}$]	**v** [$cm\ s^{-1}$]
TMD amplitudes	19	15
TMD - Wave Glider 26		
Track	3	1
Box 1	6	6
Box 2	22	9
Box 3	29	19
Box 4	10	9
TMD - Moorings		
Location 233	9	7
Location 313	4	7
Location 314	7	5

Table 3.1: RMSE for comparisons between tidal predictions for TMD and Wave Glider, and for TMD and Moorings. TMD M2 amplitudes are given for context.

3.1.2 Correlation

Using the same data sets as for the RMSE, the next statistical method applied is correlation. The results are shown in Table 3.2. The values for the entire Wave Glider track are quite high (0.98-0.99), meaning both time series are strongly correlated. The correlation decreases when splitting the data set into boxes. This could be because the time series are much shorter than for the entire track. The values for Box 3 are different from the other boxes, as the correlation for the u-velocity is much lower than the other u-velocities, and the correlation for the v-velocity is negative. Box 3 contains the almost 180° turn in direction made by the Wave Glider. The low correlation values might be caused by this turn. The correlation between the moorings and the TMD data is quite similar for each mooring.

	u	v
TMD - Moorings		
Location 233	0.91	0.88
Location 313	0.91	0.89
Location 314	0.87	0.88
TMD - Wave Glider 26		
Track	0.98	0.99
Box 1	0.95	0.95
Box 2	0.97	0.71
Box 3	0.50	-0.88
Box 4	0.91	0.96

Table 3.2: Correlation for comparisons between tidal predictions for TMD and Wave Glider, and for TMD and Moorings

3.1.3 Tidal Analysis

Next, a tidal analysis (Table 3.3) was performed on each dataset, using the t-tide function in Matlab. This was already used to create the tidal predictions used for the RMSE and correlation analyses. However, an in-depth analysis of the major and minor axes, the inclination and the phase gives more information on how well the Wave Glider is able to measure the tides. A harmonic analysis was performed on the Wave Glider data in box 1, 2 and 3 (Table 3.4). In Table 3.3, no error for the TMD dataset is given, as this dataset only includes the M2 tide. Although there might still be an error in the data, this will not appear in the tidal analysis. Table 3.3 shows that the TMD data gives higher values for the major axis than the moorings, although this difference is only significant for CM233. The same is true for the minor-axis. The other moorings only have differences of 1-2 $cm\ s^{-1}$. For the inclination and phase, differences are small, ranging from 2-4° and 2-8°, respectively. A comparison between the TMD data and Wave Glider data shows that generally, the values are similar, with differences of 0-4 $cm\ s^{-1}$ for the minor axis and 2-3° for the inclination. The major axis and phase show larger differences for box 4 (12 $cm\ s^{-1}$ and 18°, respectively). A small part of these differences is explained by the possible error (as determined by t_tide) in the Wave Glider analysis, although these errors are only 2 $cm\ s^{-1}$ for the major and minor axis, and 3° for the inclination and phase. The errors for the entire track are larger, which might be connected to the larger spatial variability (the area that the Wave Glider track covers).

	Major axis [$cm\ s^{-1}$]	**Error** [$cm\ s^{-1}$]	**Minor axis** [$cm\ s^{-1}$]	**Error** [$cm\ s^{-1}$]	**Inclination** [°]	**Error** [°]	**Phase** [°]	**Error** [°]
CM								
233	25	1	-7	1	26	2	242	2
313	20	1	11	1	67	4	231	5
314	21	1	7	1	35	3	231	3
TMD								
233	34	-	-15	-	26	-	240	-
313	21	-	9	-	71	-	239	-
314	22	-	6	-	33	-	235	-
Track	23	-	9	-	35	-	220	-
Box 1	22	-	14	-	43	-	222	-
Box 2	21	-	7	-	8	-	201	-
Box 3	26	-	4	-	15	-	239	-
Box 4	31	-	7	-	45	-	217	-
Wave Glider								
Track	21	13	10	12	33	56	208	63
Box 4	43	2	7	2	46	3	235	3

Table 3.3: Tidal Analysis for moorings, TMD and Wave Glider. Analysis was performed using t_tide in Matlab. Errors for TMD are left out, as this time series consisted entirely of the M2 tidal component, and any error that may be in there, would not be picked up truly by t_tide

As for the harmonic analysis (Table 3.4), the amplitudes for the Wave Glider and the TMD data are compared. The values are in the same order of magnitude, with a 2-5 $cm\ s^{-1}$ difference for the u-velocity, and a 3-7 $cm\ s^{-1}$ for the v-velocity. However, when looking back at Figure 2.2, the tidal ellipses in this box mainly extend in the u-direction, and show little amplitude in v-direction.

	Wave Glider		**TMD**	
	u [$cm\ s^{-1}$]	v [$cm\ s^{-1}$]	u [$cm\ s^{-1}$]	v [$cm\ s^{-1}$]
Box 1	21	23	18	18
Box 2	25	1	20	8
Box 3	26	16	24	13

Table 3.4: Harmonic Analysis for box 1, 2 and 3 for Wave Glider data and TMD data.

The final step of the tidal analysis is investigating how much of the variability is explained by the tides (Table 3.5 and 3.6). For the TMD data, this is 100%, since the data consists of only the M2 tidal component. For the moorings, a large part of the variability, 73-85%, is explained by the tides. The variability in the Wave Glider data is only 26% explained by the tides, however, this number increases when the spatial variability is decreased, which is clear in box 4, with 86%. With the harmonic analysis, different values are determined for u and v. The values for the u-velocity are all between the values for the entire track and Box 4, so, when the area covered by the Wave Glider decreases, less noise is present, and the percentage of variability explained by the tides is larger. However, the values for the v-velocity are different, especially for Box 2.

Moorings	%
Location 233	73
Location 313	83
Location 314	85
Wave Glider	
Track	26
Box 4	86

Table 3.5: Percentage of variability explained by the M2 tide according to the tidal analysis performed using t_tide. This shows the amount of the variability (in the time series) that was caused by the M2 tidal constituent.

	Wave Glider		TMD	
	u [%]	v [%]	u [%]	v [%]
Box 1	46	55	91	91
Box 2	69	0	91	91
Box 3	59	30	91	91

Table 3.6: Percentage of variability explained by the M2 tide according to the harmonic analysis. This shows the amount of variability (in the time series) that was caused by a tidal component with a 12.5 hour period.

The last step in determining the quality of the Wave Glider data is a visual analysis of the measurements. In Figures 3.3, 3.4 and 3.5, AMM7 data is presented, along with the Wave Glider measurements. Figure 3.5 shows the de-tided current velocities from the Wave Glider, along with the mean current velocity calculated from AMM7 values. Overall, the Wave Glider shows similar results to AMM7, the direction of the vectors is alike, the magnitude is, especially after the sharp turn, often too high (0.7 $m\ s^{-1}$, whereas AMM7 is 0.3 $m\ s^{-1}$). At the most northern point of the track, the direction of the velocities turns approximately 180°. At this point, the Wave Glider itself also turns, so this might interfere with the measuring of the velocities. The Wave Gliders also show similar values for temperature and salinity, with some variations (Figure 3.3 and 3.4). For the salinity, these variations can be as large as 0.5. The variations in temperature are between 0.25 – 0.50 °C. The standard deviation of the AMM7 data shows that there is barely any variability in the salinity in this area, although there are some small variations (with a maximum of 1.5%) near the coast. The temperature shows larger variations, of up to 5%.

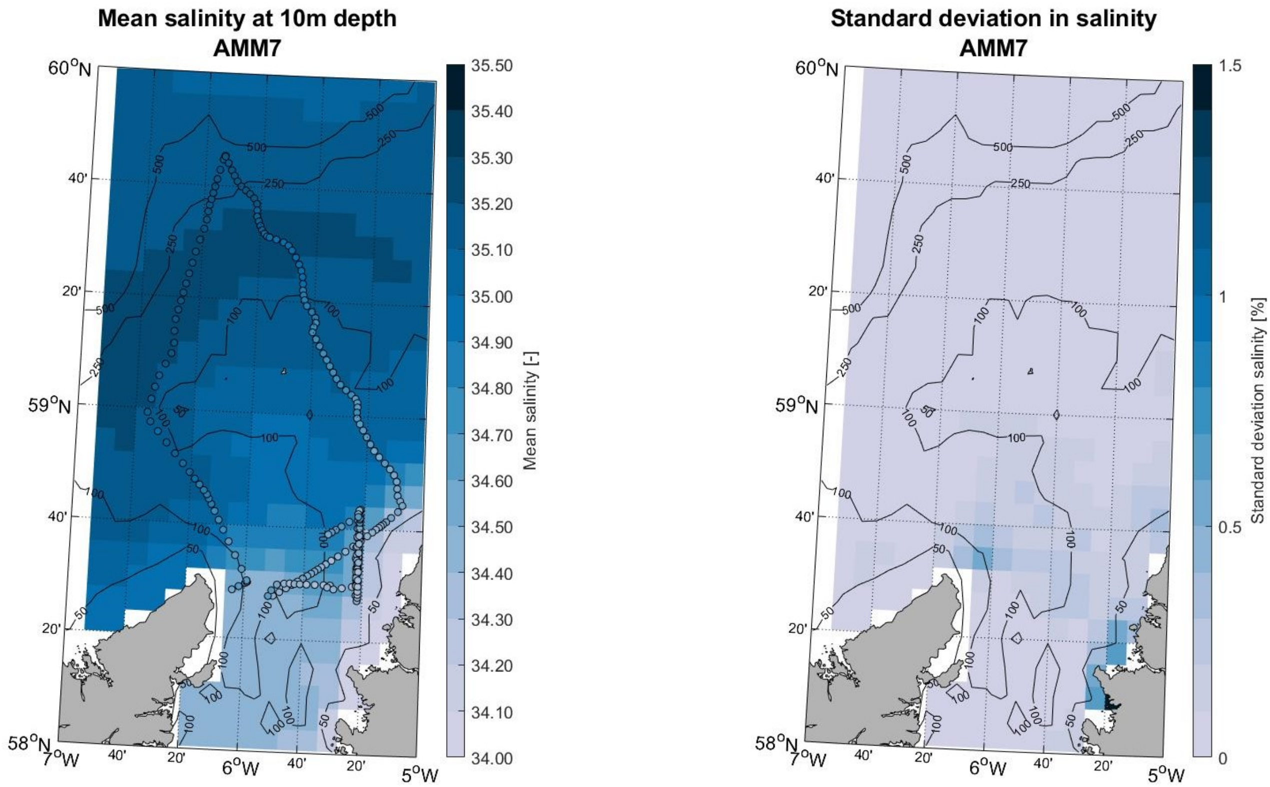

Figure 3.3: left: Salinity measurements Wave Glider and mean salinity AMM7. Salinity from AMM7 is an average of the entire Wave Glider deployment period (September 19th - 30th). right: Variation in salinity AMM7, during the same period. This shows the variation, as a percentage of the mean, for the AMM7 salinity during the Wave Glider deployment, calculated using a standard deviation function.

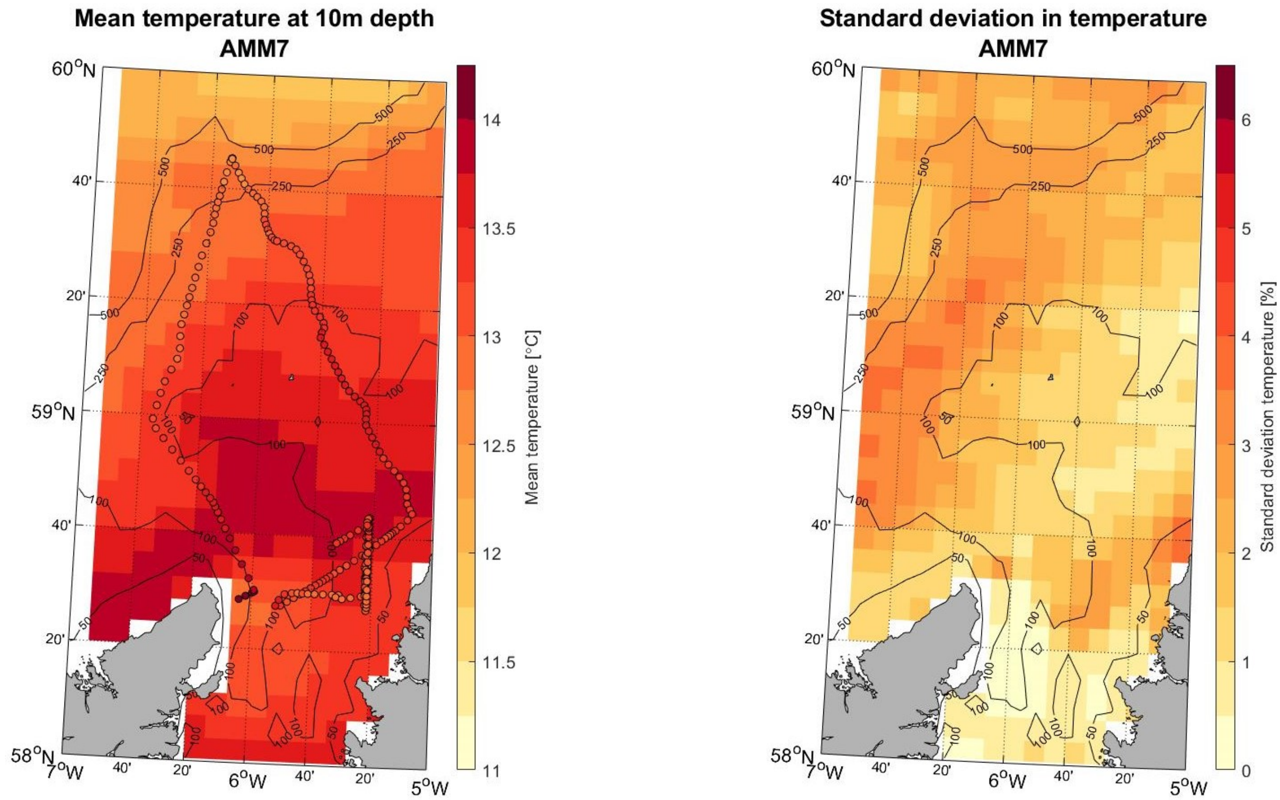

Figure 3.4: left: Temperature measurements Wave Glider and mean salinity AMM7. Temperature from AMM7 is an average of the entire Wave Glider deployment period (September 19th - 30th). right: Variation in temperature AMM7, during the same period. This shows the variation, as a percentage of the mean, for the AMM7 temperature during the Wave Glider deployment, calculated using a standard deviation function.

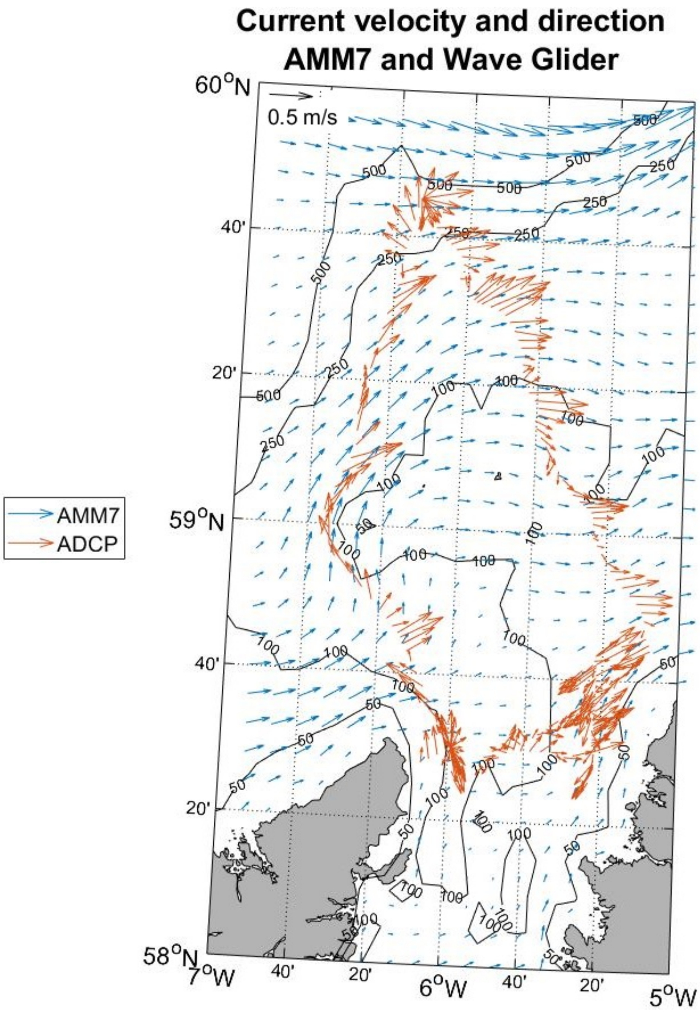

Figure 3.5: De-tided measured current velocities Wave Glider and average de-tided current velocities AMM7. Current velocities for AMM7 are averaged over the entire Wave Glider deployment period (September 19th - 30th). The black arrow in the top left corner shows the scale of the arrows.

3.2 SQ2: Circulation

For the second sub-question, the focus is on calculating the transport across some sections in the study area, using the AMM7 data, and determining the cause of the variability by comparing it to meteorological data. First, however, the transport on one of the Wave Glider sections is calculated using both the AMM7 data and the Wave Glider transport. In Figure 3.6, this transport can be seen, as well as the AMM7 mean and standard deviation. It should be noted that this 'standard deviation' refers to the variability of the daily transport, which is calculated as the standard deviation from the mean transport over these 11 days. The assumption here is that the standard error of the AMM7 values is smaller than the variation during this time. This also applies for the following sections (the monthly or annual variation). The transport calculated using the Wave Glider is slightly lower (0.95 Sv) than the mean AMM7 transport (1.1 Sv), but within the boundaries of the variability of the AMM7 transport.

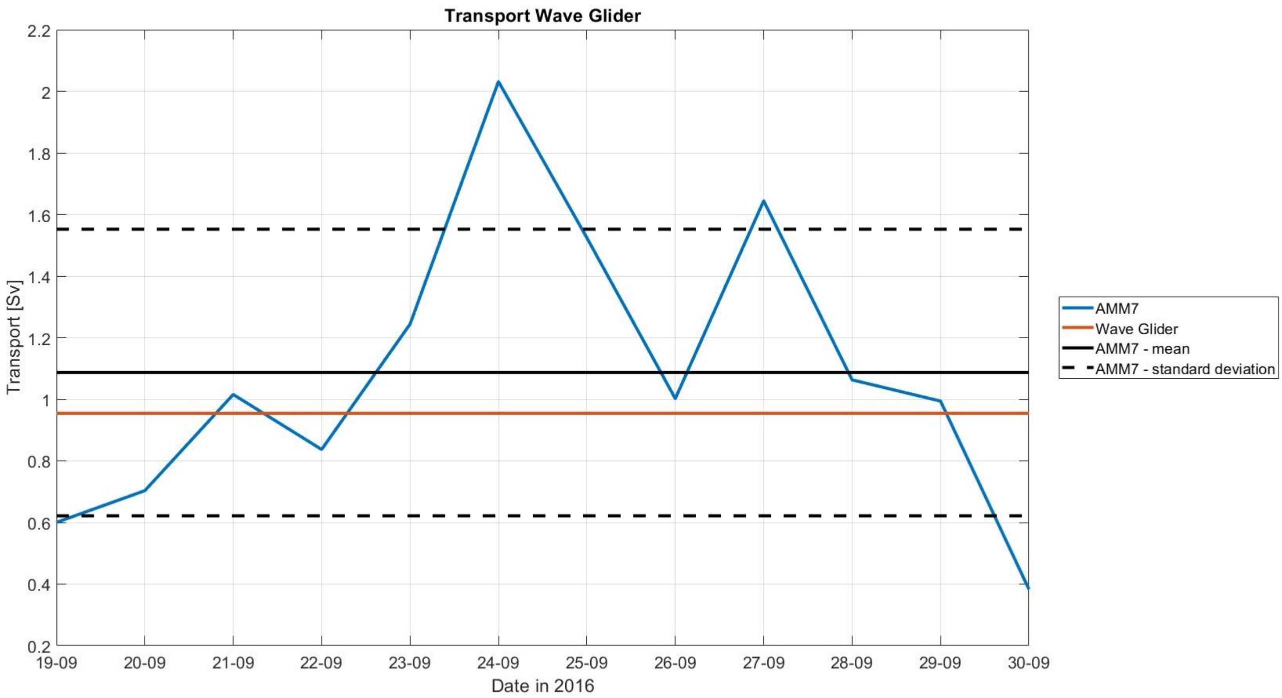

Figure 3.6: Transport calculated with Wave Glider measurements and with AMM7 data. The Wave Glider measurements were taken between September 22nd - 25th, AMM7 calculations are based on entire Wave Glider deployment (September 19th - 30th. Variation (calculated as standard devation from the mean) and average transport of AMM7 are also presented.

Figure 3.7 shows the monthly and weekly average transport across Shelf-4, the North Minch, Shelf-3 and Shelf-2. It shows a decrease in transport from Shelf-4 to Shelf-3 (from an average of 1.1 Sv, to 0.75 Sv), and then an increase to Shelf-2 (to 1.6 Sv). Also, variability in winter (approximately 1 Sv on Shelf-4) is higher than in summer (less than 0.5 Sv (Shelf-4)). The weekly variability is quite high, with amplitudes up to 1.5 Sv in winter, and 0.5 Sv in summer. Monthly variability is much lower, with amplitudes of less than 1.0 Sv in winter, and a quite constant transport in summer. As Figure 3.8 shows more clearly, variability in transport across the North Minch is of a lower order than across the Shelf sections. The Shelf sections also all show a significant dip in transport in November.

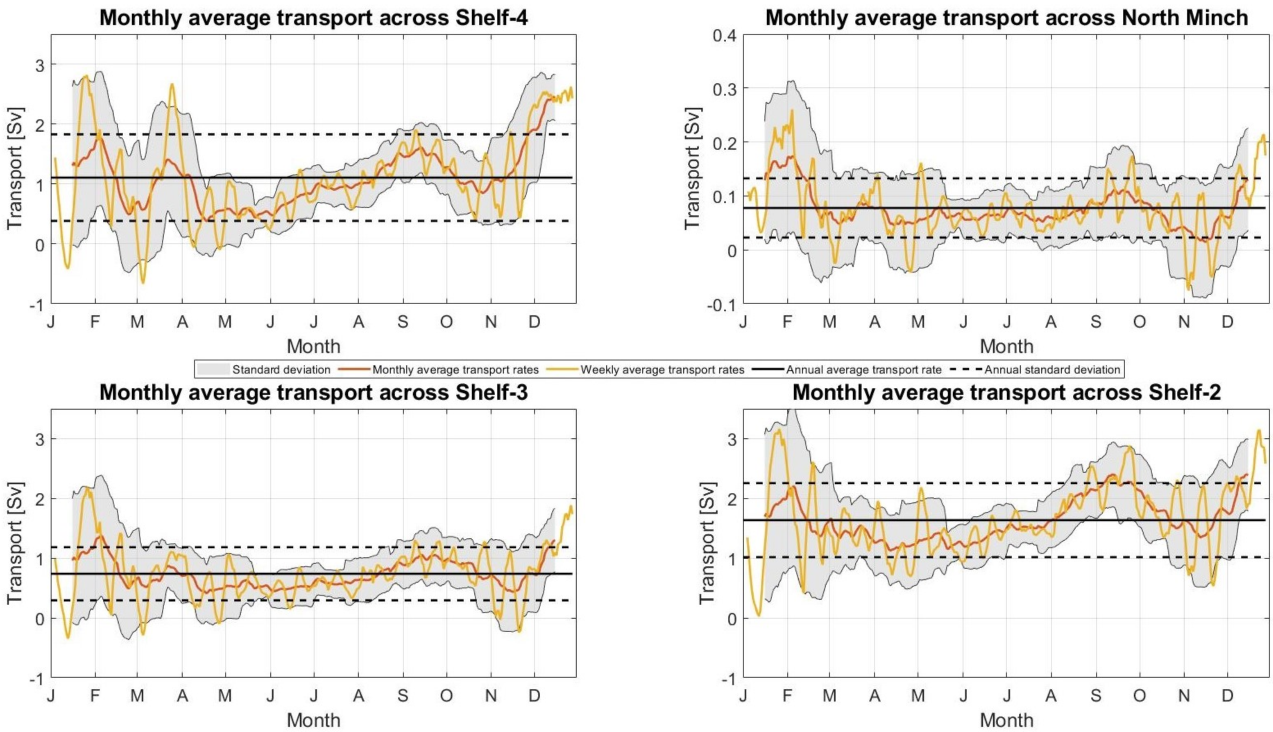

Figure 3.7: Weekly and monthly transport (Sv) for sections Shelf-4, North Minch, Shelf-3 and Shelf-2, calculated using the AMM7 data set. The monthly variability (calculated as standard deviation from the mean) is also presented, as well as the annual mean and variability. The red lines represent the monthly averaged transport, the yellow lines represent the weekly averaged transport. The grey shading shows the daily variability. The solid black lines indicate the annual mean, and the dashed lines represent the annual variability.

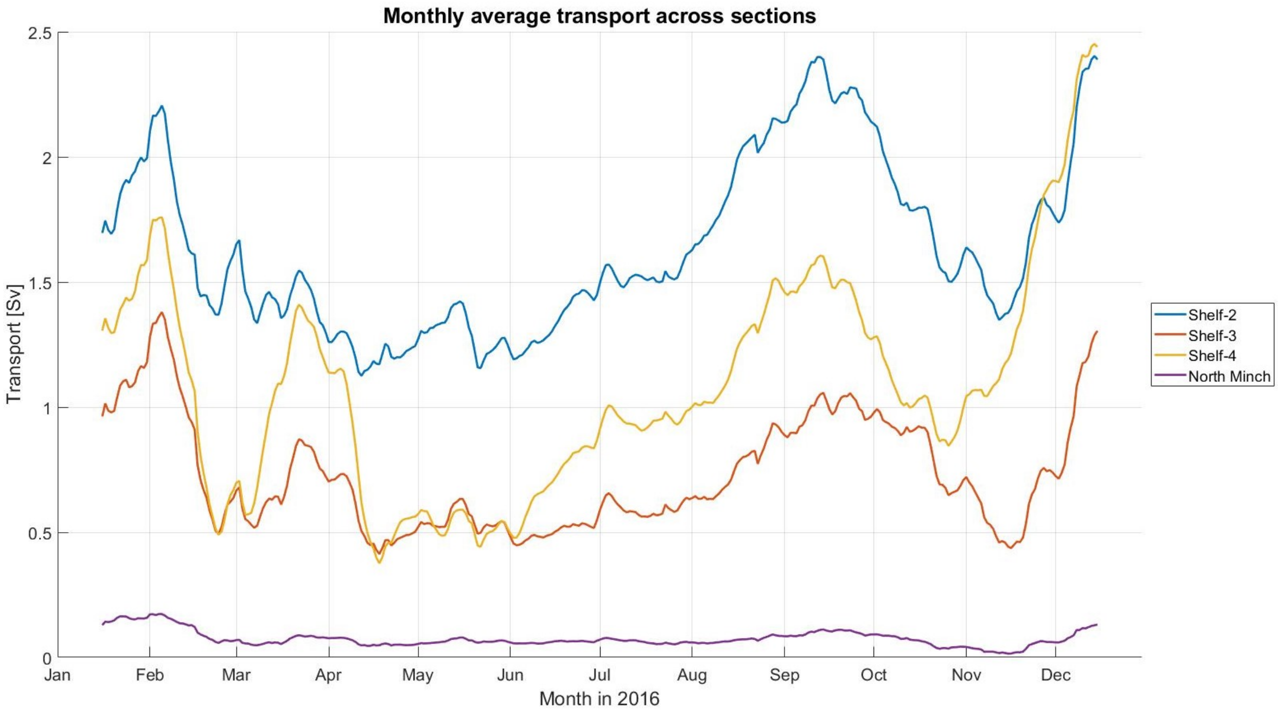

Figure 3.8: Monthly transport (Sv) for sections Shelf-4, North Minch, Shelf-3 and Shelf-2, calculated using the AMM7 data set.

Both Figure 3.7 and 3.8 show an increasing transport between summer (July) and winter (December), with the exception of the month November. In November, transport across all sections is quite low when compared to October (a decrease of 0.6-1.0 Sv for Shelf-4, Shelf-3 and Shelf-2). In December, the transport increases again, with increases varying between 0.9-1.5 Sv. When the transport in November is studied more closely, it shows that overall, the transport is lower than September, October and December. Early in November, the highest transport is 1.5 Sv, whereas in early October, averages are around 2.0 Sv, and in December, these values rise to 2.5 Sv. Later on in November, the highest transport also reaches 2.5 Sv. There are two events in November contributing to a lower average transport: one around the 6^{th} of November, and one from the 19^{th} to the 22^{nd} (Figure 3.9). To determine the cause of these events, the wind speed, wind direction and surface air pressure in the region are plotted in Figures 3.10 and 3.11.

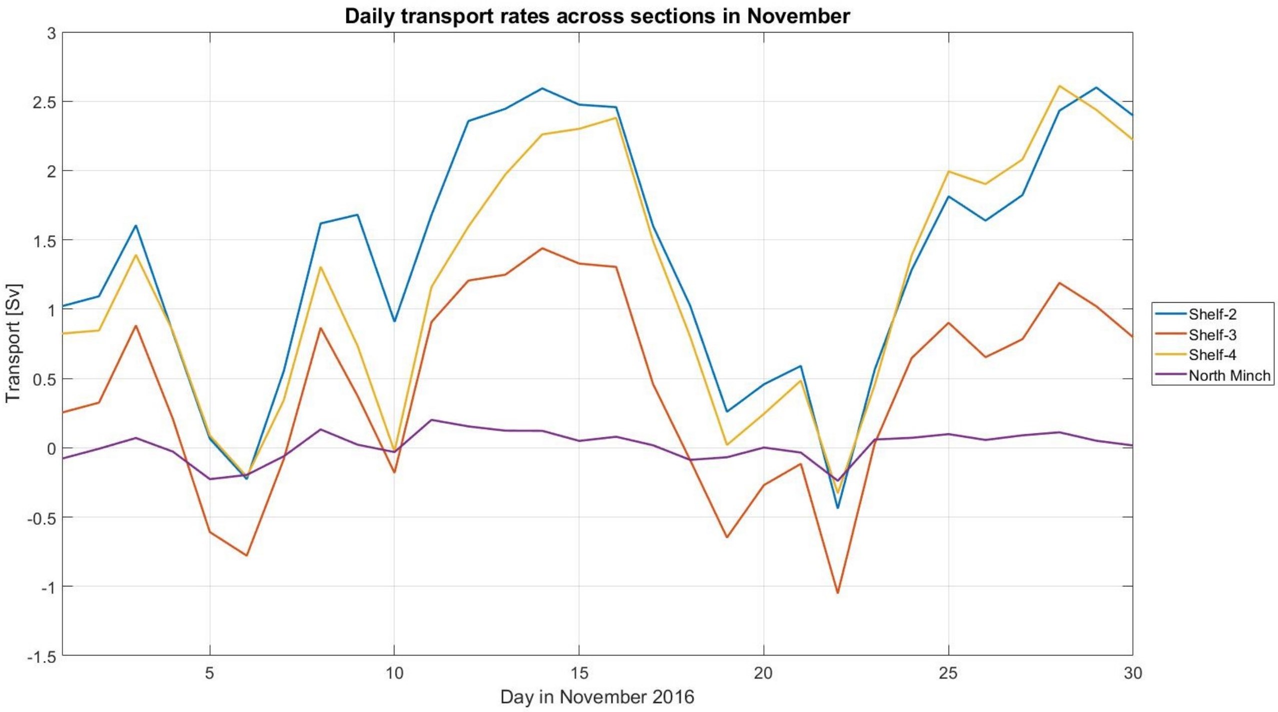

Figure 3.9: Daily transport (Sv) in November, calculated using the AMM7 data set. Transport across the North Minch section remains quite constant, but the other sections show two clear events, one around the 5^{th}, and one around the 20^{th}.

Both events correspond to increases in wind speed and changes in wind directions. In Figure 3.10, these increases and changes are clear on the $4^{\text{th}}/5^{\text{th}}$ and the 22^{nd} of November. At the 4^{th}, the wind direction shifts from southwest to northeast, so directed against the transport direction. The wind speeds increase from approximately 3 $m\ s^{-1}$ on the 3^{th} to 10 $m\ s^{-1}$ on the 5^{th}. Between the 20^{th} and the 22^{nd}, the wind speed shows a small increase from 2 $m\ s^{-1}$ to 7 $m\ s^{-1}$. A decrease in surface air pressure is present just before each event, at the 4^{th} and at the 17^{th}. The surface air pressure decreases from approximately 10.2 dbar to just under 10.1 dbar between the 3^{rd} and the 5^{th}, and from just over 10.1 dbar on the 15^{th} to approximately 9.85 dbar on the 17^{th}.
As a final step for this sub-question, the water masses are investigated. Several T-S diagrams are produced, categorised by either depth, distance from the coast, or month of the year. In these diagrams, a line of constant salinity of 35.0 is used to define the upper bound of the Scottish Coastal Current (SCC). Two boxes are used to represent NAW and MNAW. In the

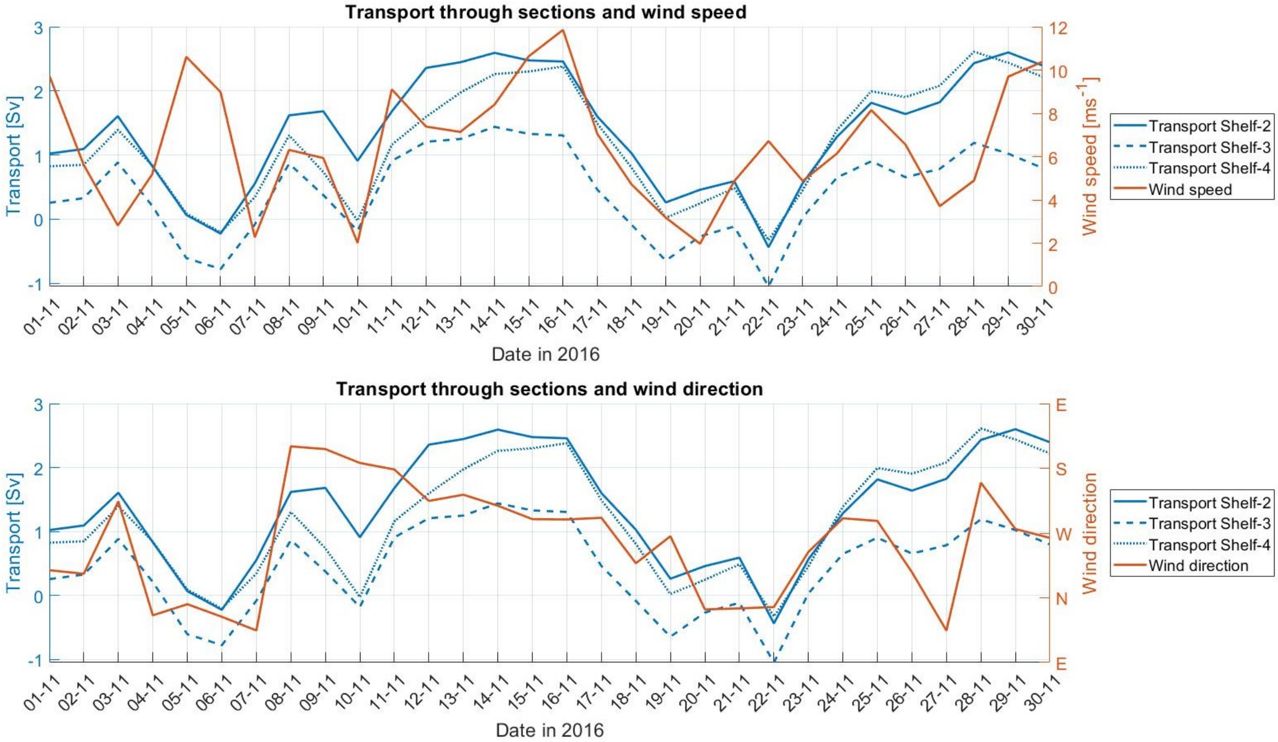

Figure 3.10: Wind speed ($m\ s^{-1}$; upper; orange line; right hand axis) and direction (lower; orange line; right hand axis) in November, and transport (Sv; blue lines; left hand axis) through sections Shelf-4, Shelf-3 and Shelf-2. Transport across the North-Minch remained quite constant through both events and is therefore not depicted in these figures.

plots categorised by depth and month, the Wave Glider results are also added. Figure 3.12 shows that generally, colder, more saline water is found at deeper locations, and warmer, fresher water is found at the surface. The salinity measured by the Wave Gliders varies, but the temperatures found are all in the upper region of the temperature range (13-14°C), where they are expected. The salinity increases with distance from the coast (Figure 3.13). Salinity for the section across the North Minch is lower compared to the other sections, with most values under 35.0. The salinity appears to be stable throughout the months, varying between 34.2 and 35.3 (Figure 3.14), while seasonal heating is very clear, with the coldest temperatures found at the end of the winter, and highest temperatures at the end of summer.

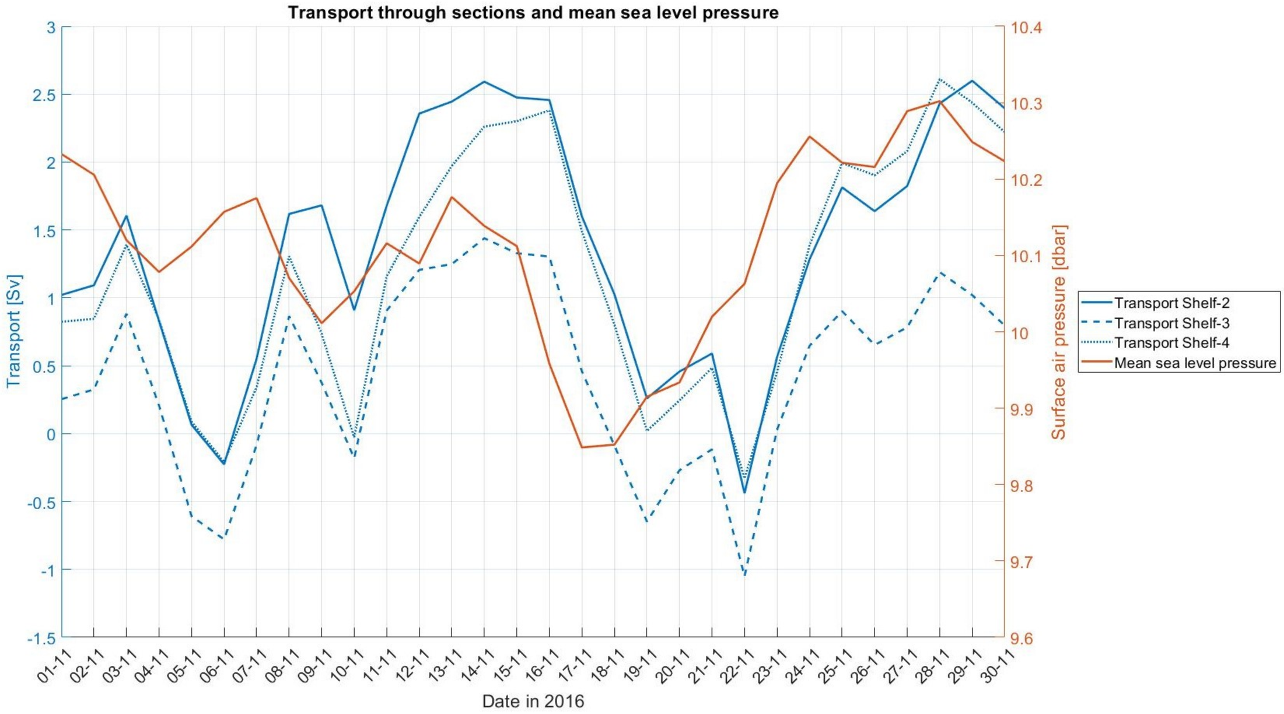

Figure 3.11: Mean sea level pressure (dbar; orange line; right hand axis) in November, and transport (Sv; blue lines; left hand axis) through sections Shelf-4, Shelf-3 and Shelf-2. Transport across the North-Minch remained quite constant through both events and is therefore not depicted in these figures. There might be a possible lag between the sea level pressure and the transport.

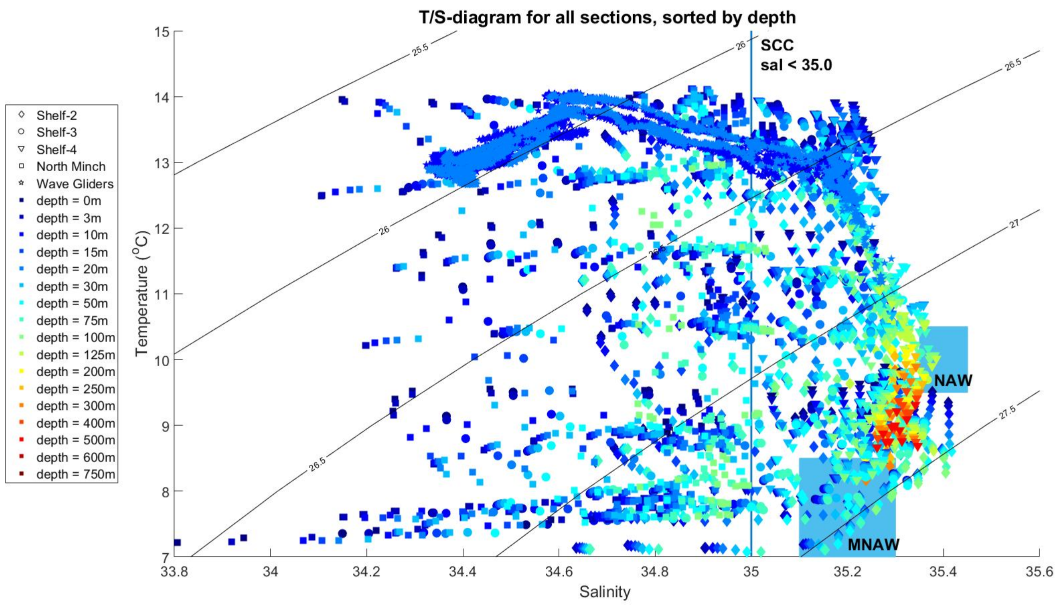

Figure 3.12: T-S diagram. Five different markers represent the four sections (AMM7 data) and the Wave Glider data. The colours indicate the depth of the measurement. A line at a salinity of 35 marks the upper bound of the Scottish Continental Current. Blue squares represent the typical characteristics for the MNAW and NAW water masses. The diagonal lines are lines of equal density in $kg\ m^{-3}$

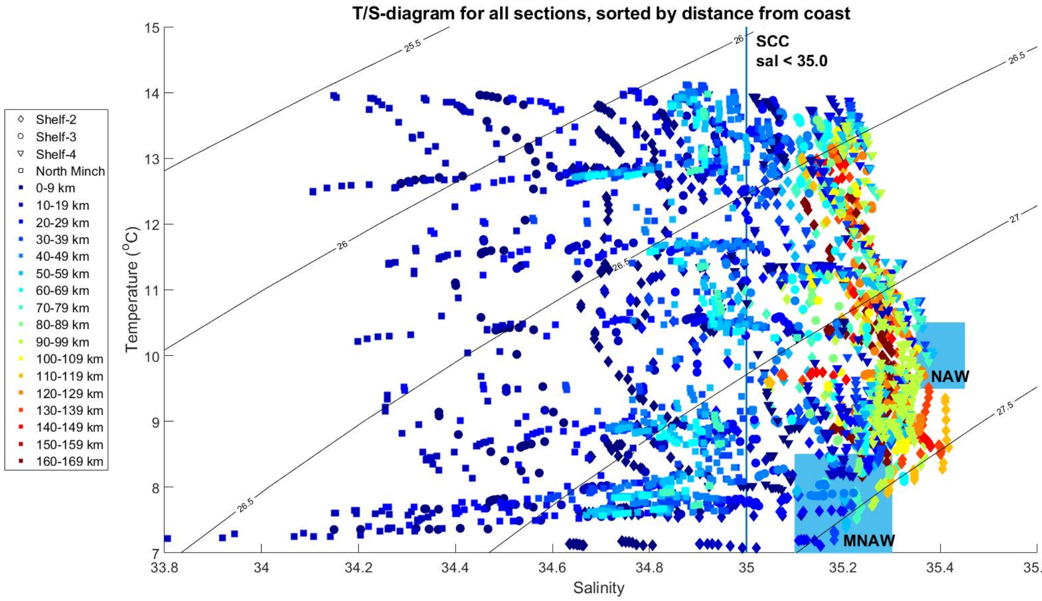

Figure 3.13: T-S diagram. Similar to Figure 3.12, but here colours indicate the distance to the coast.

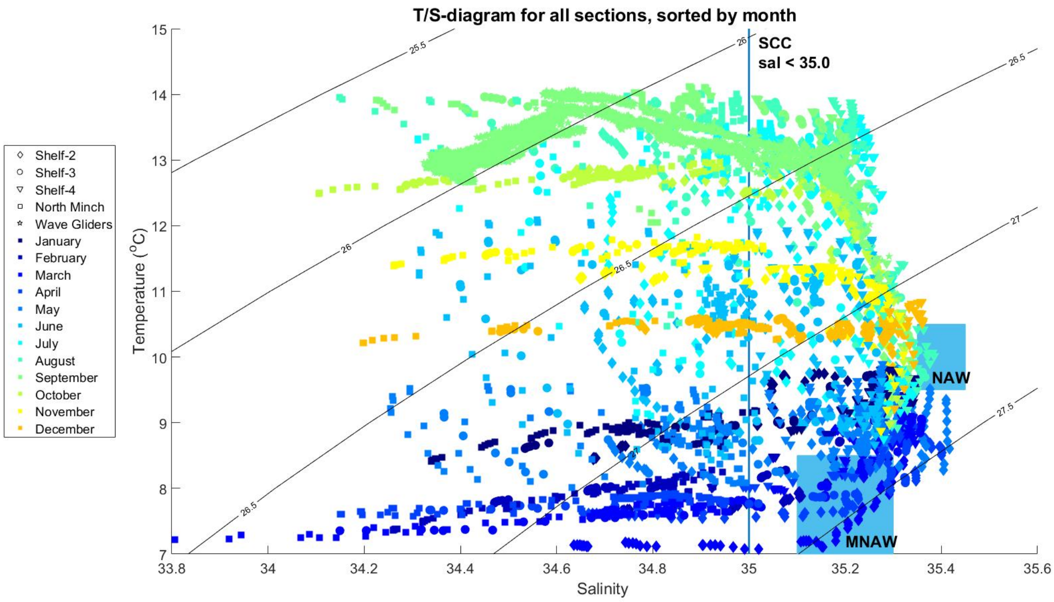

Figure 3.14: T-S diagram. Similar to Figure 3.12, but here colours indicate the month in which the measurement was taken.

To determine differences between the sections, the average temperatures and salinities are shown in Table 3.7. The salinity is lowest at the North Minch, and highest at Shelf-4. Considering that transport through the North Minch section consists mostly of Scottish Coastal Current water, and not much Atlantic Inflow, the lower salinity makes sense. The temperature is highest at Shelf-4, and decreases northward.

Section	Mean temperature [°]	Mean salinity [-]
Shelf-4	10.51	35.22
North Minch	10.48	34.76
Shelf-3	10.49	35.04
Shelf-2	10.18	35.10

Table 3.7: Mean temperatures and salinities for Shelf-4, North Minch, Shelf-3 and Shelf-2, based on AMM7 data

3.3 SQ3: Transport on the main path of Atlantic Water from the shelf edge to the North Sea

To answer the third sub-question, the weekly running averages and standard deviations for the Ellet Line, Shelf-4, Shelf-0, Fair Isle Gap, North-Shetland and Feie-Shetland sections were calculated (Figure 3.15 and 3.16). The variability for all sections is highest in winter and lowest in summer, although this is more clear for the Ellet Line, Shelf-4, Shelf-0 and North-Shetland. The mean transport increases from the Ellet Line to Shelf-0, from approximately 0.5 ± 0.4 Sv to 3.2 ± 0.7 Sv. Figure 3.16 shows the weekly average transport of all sections. It shows that most sections have similar signals ,with the largest peaks and drops followed by all sections. Also, the extremity of the variations in summer is lower than in winter. This can be seen in the standardized transport (Figure 3.17). However, Feie-Shetland shows some irregularities. It shows some drops where the other sections show peaks. This might be due to the fact that transport through this section is not only determined by the currents flowing through the other sections, but also by the Norwegian Coastal Current.

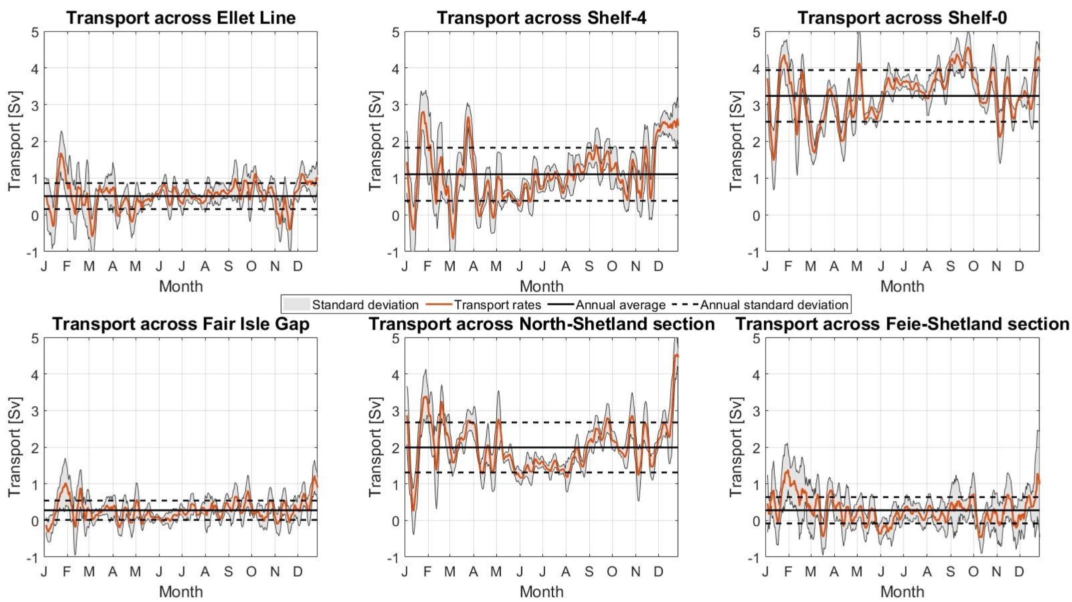

Figure 3.15: Weekly averaged transport (Sv) through Ellet Line, Shelf-4, Shelf-0, North Shetland, Fair Isle Gap and Feie-Shetland , based on AMM7 data. Orange line show weekly transport, grey shading shows daily variability. Black solid line represents annual mean, and the black dashed line the annual variability (calculated as standard deviation from the mean).

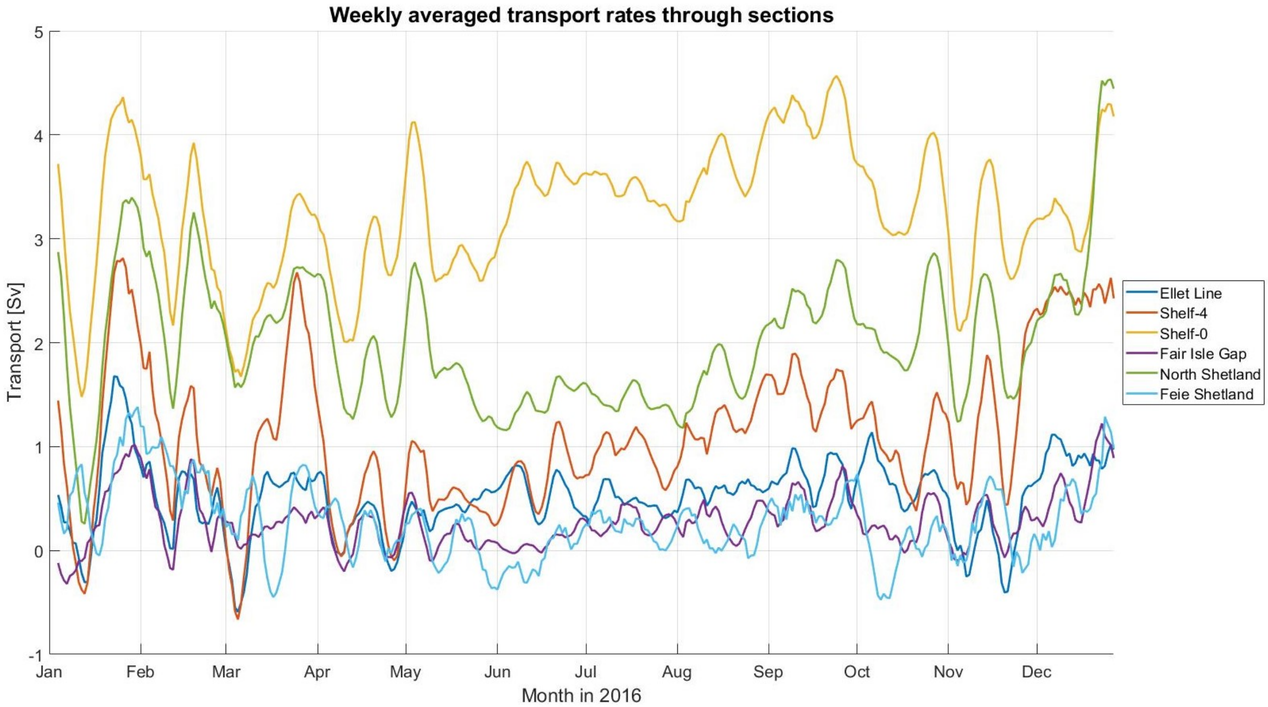

Figure 3.16: Weekly averaged transport (Sv) through Ellet Line, Shelf-4, Shelf-0, North Shetland, Fair Isle Gap and Feie-Shetland , based on AMM7 data.

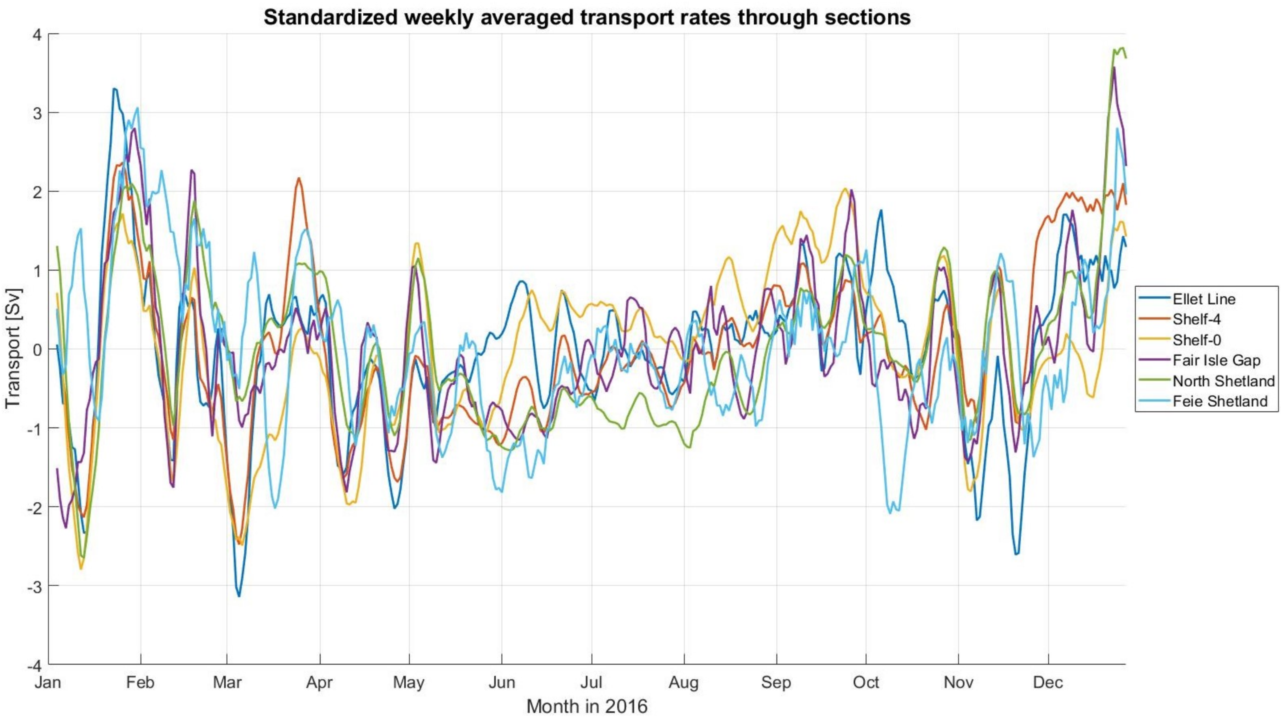

Figure 3.17: Standardized weekly averaged transport through Ellet Line, Shelf-4, Shelf-0, North Shetland, Fair Isle and Feie-Shetland , based on AMM7 data. The data is standardized by subtracting the mean and dividing by the standard deviation of each times series.

To study the propagation of the signals between the sections, the lags, relative to the Ellet Line, are determined using cross-correlation. The calculations reveal a lag of 0 days from the Ellet Line, except for the Feie-Shetland section, which has a lag of 4 days according to the calculation. The cross-correlation at these lags are shown in Table 3.8. The cross-correlation with respect to the Ellet Line decreases with greater distance. For Feie-Shetland, the cross-correlation is low (0.21) at the lag of 4 days. Figure 3.18 shows only the transport on the Ellet Line and the Feie-Shetland section. In this figure, a small lag is sometimes visible (for example, the peak at the end of January). However, there is also a lot of variation between the two sections, so some signals might have a different origin.

Section	**Lag [days]**	**Cross-correlation at lag**
Shelf-4	0	0.79
Shelf-0	0	0.60
Fair Isle Gap	0	0.56
North Shetland	0	0.51
Feie-Shetland	4	0.21

Table 3.8: The lag with respect to the Ellet line for each section, calculated using the cross-correlation. The correlation at this lag is also given.

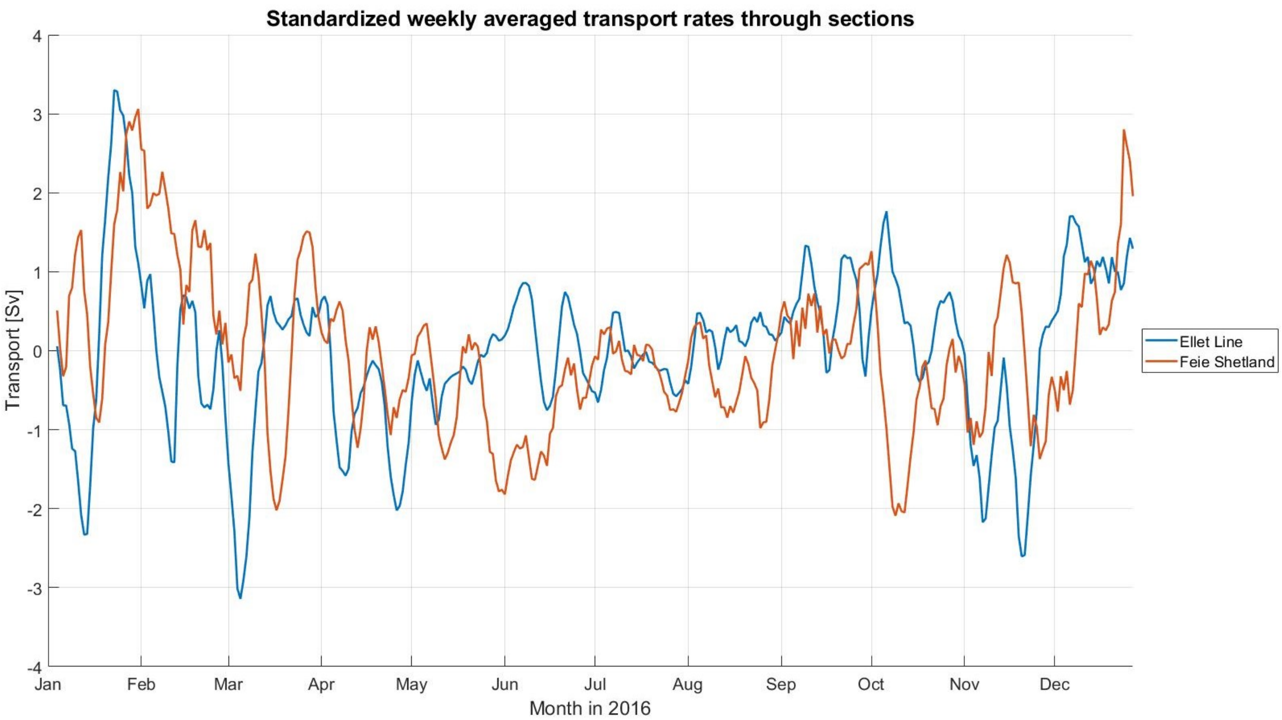

Figure 3.18: Standardized weekly transport for the Ellet Line and the Feie-Shetland section. Similar to Figure 3.17.

Chapter 4

Discussion

In this chapter, the results are interpreted and discussed. This discussion is sorted by physical processes. First, the Wave Glider's ability to distinguish the tides is discussed. Then, the circulation on the shelf is explained. Finally, the variability along the path of Atlantic Water from the shelf edge into the North Sea is studied.

4.1 Wave Glider data quality

The RMSE and correlation analysis show that the Wave Glider overall seems to be able to distinguish the M2 component of the tides, when compared to the TMD data. The averaging of the 14 TMD locations along the Wave Glider track might account for the spatial variability of the Wave Glider data. The RMSE increases when the track is split into boxes, while the correlation decreases. While the spatial variability decreases, the time series length also decreases, which makes the tidal prediction less precise.

Box 3 has high RMSEs and low correlation values (29/19 $cm\ s^{-1}$ and 0.50/-0.88, respectively). This might be due to the fact that the Wave Glider makes a turn, from heading northeast to heading southeast, leading to unreliable measurements (Figure 3.5).

Box 1 and 4 have lower RMSEs than Box 2 and 3 (6-10 $cm\ s^{-1}$ compared to 9-29 $cm\ s^{-1}$). Box 4 covers 3 days, leading to a longer time series. Since Box 4 is part of box 1, box 1 also has a longer time series, making the tidal prediction more precise.

Overall, the Wave Glider also seems to do all right in the tidal analysis. For Box 4, the major axis and phase are overestimated by 12 $cm\ s^{-1}$ and 18°, respectively, compared to the TMD. The minor axis and inclination are similar to the TMD results. The combination of spatial and temporal variation in the entire Wave Glider track seems to have an effect on the phase, but not on the other parameters. The percentage of variability explained increases with decreasing spatial variability. Box 4 has the lowest spatial variability, and the tides account for 86% of the variability in the time series. For the entire track, this is only 26%. The other boxes have percentages between this. This might indicate that a higher spatial variability (a longer track, or greater area covered by the Wave Glider) can lead to more variability or noise in the time series.

In the visual analysis, the current velocity seems to be measured accurately. It follows the topography, on the straight sections. However, in the turning points, the velocity directions turn with the turning of the Wave Glider. This would mean that the Wave Glider is reliable on straight sections, but not when changing direction. Also, after turning, the Wave Glider gives higher velocity values than the AMM7 data. It might be that this difference is caused by the averaging of the AMM7 data, but it could also be that the Wave Glider overestimates the velocity.

Moving northwards, the salinity measurements are similar to the AMM7 values, with variations of 0.1. However, moving southwards, towards the west coast of Scotland, the Wave gives lower values, with a maximum difference of 0.5. This might be because the Wave Glider underestimates the salinity, but could also be caused by the grid size of the AMM7 model. The higher salinity area just above 58 °N might be intrusion from the slope onto the shelf. Figure 4.1 shows that this higher salinity area starts just at the slope edge. The variability (standard deviation from the mean) in the salinity is overall quite low (0 – 0.5%, with some larger variations along the coast (up till 1.5%). These variations are likely caused by freshwater inflow from the rivers. However, the coarse grid of the AMM7 model also causes some extra uncertainty, especially near the coast.

The temperature measurements from the Wave Glider seem to be similar to the AMM7 data, although maybe slightly overestimated at some points, with differences between 0.25 and 0.50 °C. This could be caused by small temporal variations due to solar heating. Because these measurements are only at 8 metres depth, solar heating plays a large role in the seasonal and local heating. The higher temperatures near the coast might be caused by this local heating, but the larger domain shown in Figure 4.2 also indicates that this might originate from the warmer waters on the Malin Shelf.

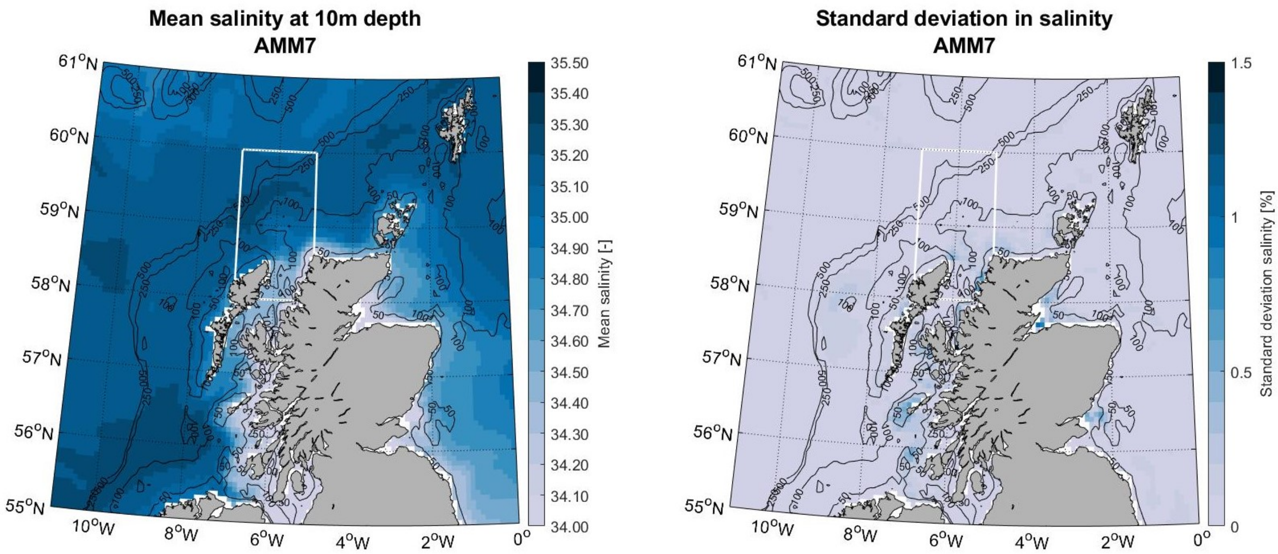

Figure 4.1: Larger domain salinity from AMM7 data. In both figures the study area is represented by a white rectangle. Left shows the mean salinity, averaged over the Wave Glider deployment period (September 19th - 30th). Right shows the variability in salinity during this period, calculated as the standard deviation from the mean, in percentages of the mean.

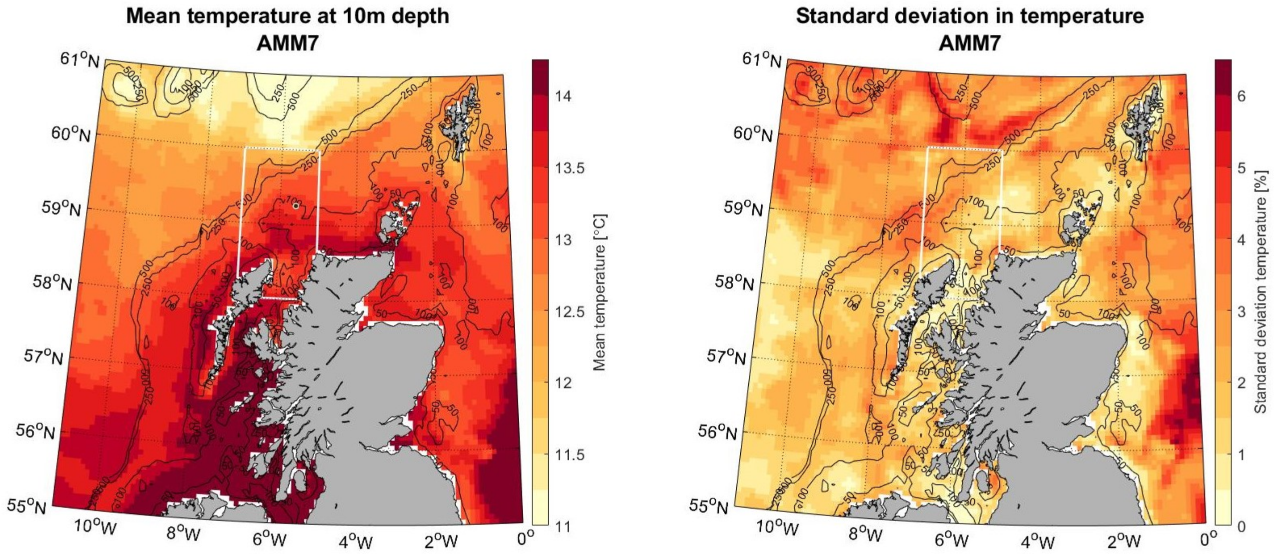

Figure 4.2: Larger domain temperature (°C) from AMM7 data. In both figures the study area is represented by a white rectangle. Left shows the mean temperature, averaged over the Wave Glider deployment period (September 19th - 30th). Right shows the variability in temperature during this period, calculated as the standard deviation from the mean, in percentages of the mean.

4.2 Transport on the shelf

4.2.1 Transport across sections

Figure 3.7 shows an increase in transport between Shelf-3 and Shelf-2, from 0.75 Sv to 1.6 Sv. Figure 1.3 shows an inflow of Atlantic Water onto the shelf. This inflow might explain the increase in transport. According to Huthnance et al. (2009), westerlies tend to drive on-shelf surface flow from the slope at 60° N. This would support the theory that the increase in transport is caused by the Atlantic Water inflow. This is also indicated by the sections used to determine the variability of the transport of Atlantic Water from the shelf edge into the North Sea. The transport increases from south to north, from 0.5 ± 0.4 Sv at the Ellet Line, to 3.2 ± 0.7 Sv at Shelf-0. Here, a sharp increase between Shelf-4 (1.1 ± 0.7 Sv) and Shelf-0 is seen. To analyse whether this is caused by Atlantic Water inflow, a temperature cut-off might be necessary to filter out Atlantic Water.
Another reason might be that Shelf-2 is significantly longer than Shelf-4 and Shelf-3 (lengths are 167 km, 95 km and 121 km, respectively), and therefore the velocities are multiplied by a greater area. However, Shelf-0 is shorter than Shelf-2 (137 km), whereas the transport across this section is twice as high.

Transport through the Minch is quite low and stable compared to the other sections. The transport through the Minch is comparable to the 0.09 transport for the Little Minch found by McKay et al. (1986) (described in Hill et al. (1997)). Shelf-4, -3 and -2 are more exposed than the North Minch section, which might cause the higher variability on these sections (0.7, 0.4, 0.6 and 0.1 Sv, respectively). The same goes for the Ellet Line, Shelf-4 and Shelf-0, which are more exposed to conditions on the Atlantic Ocean than the Fair Isle Gap, North Shetland and Feie-Shetland, and therefore experience more pronounced variations.
The variabilities for all sections are higher in the winter than in summer. This is explained by the fact that in winter, more storms occur, leading to short-term transport variations. In summer, the weather is often more stable.

The Ellet Line used here is only a small part of the Extended Ellet Line, as studied by Holliday et al. (2015). They used almost 40 years of hydrographic measurements in the Rockall Trough and 18 years of new data from the Iceland Basin and the Hatton-Rockall Basin. They found a transport of 2.3 ± 1.3 Sv in the upper waters of the Ellet Line from the Scottish coast to the Rockall Trough. They separated the northward flowing transport into two currents, and found the slope current to be 1.8 ± 0.4 Sv. This is much higher than the transport on the Ellet Line found in this study (0.5 ± 0.4). This difference might be caused by the fact that the Ellet Line in this study was chosen as a straight line between the southern tip of the Western Isles and the shelf edge. Therefore, the section did not extend onto the slope, and would probably not include the (entire) slope current.

Turrell et al. (1990) found that the FIC mostly results from wind forcing, but that in September, when the water column is still stratified, also a non-wind-driven component is present. They found transport resulting from the FIC to be 0.13 Sv west of Orkney, and 0.4 Sv in the North Sea. During winter, the latter decreased to 0.15 Sv. In this study, transport through the Fair Isle Gap was found to be 0.3 ± 0.3 Sv. If it is assumed that the FIC increases from west of Orkney to the North Sea, these values are in line with that theory.

Transport on the Feie-Shetland section consists of several transport paths going in different directions (Figure 1.3). According to Huthnance et al. (2009), “Atlantic Water” inflows (SCS, FIC) and a transport along the continental slope add up to a total of 1.7 Sv moving into the North Sea. The Norwegian Coastal Current (NCC) transports 1–2 Sv northwards, out of the North Sea. These currents all cross the Feie-Shetland section. In this research, a mean transport of 0.3 ± 0.4 Sv was found moving northwards through the Feie-Shetland section. This is in accordance with Huthnance et al. (2009). The transport through this section is determined quite equally by the transport from the Atlantic Ocean and the NCC, which might cause the difference between signals on the other sections and this section. Splitting the section in two parts, with the Norwegian Trench as the splitting point could help with future analysis. Due to time-issues, this was not included in this research.

4.2.2 Transport in November

According to Huthnance (1997) and Holt and Proctor (2008), transport is strongly influenced by external forcing by wind, density and ocean. This is in accordance with the findings in this research, as the lower average transport in November (Shelf-4, Shelf-3 and Shelf-2) was caused by two events with low transport: around November 6th and between November 19th and 22nd. For both these events, a clear drop in surface air pressure is visible in Figure 3.11, although the drop in air pressure on the 17th is more significant (10.1 dbar on the 15th to 9.85 dbar on the 17th) than the one on the 4th (10.2 dbar on the 3rd to 10.1 dbar on the 5th). Both events also show an increase in wind speed (7 $m\ s^{-1}$ for the first event, and 5 $m\ s^{-1}$ for the second) and a change in wind direction from southwest to north-northeast, which is against the transport direction. From weather reports issued by the UK Met Office (2016), the difference between these two events becomes more clear.

- Event 1 (November 5th-7th):
  - On the 5th, there are strong winds in the North East of the UK, with local coastal gales in eastern Scotland.
  - On the 6th, there are strong winds and near gale force gusts along the eastern coasts.

– On the 7^{th}, it is still windy in the south-east, but there are lighter winds in the north-east.

- Event 2 (November 19^{th}-22^{nd}):
  – The drop in air pressure on the 17^{th} may indicate the arrival of storm Angus.
  – On the 19^{th}, storm Angus actually arrives in the south-west of the UK, causing strong winds.
  – On the 20^{th}, Angus moves eastwards along the English Channel, causing gusts of 60 knots.
  – On the 21^{st}, wind speed increases through the Irish Sea.
  – Finally, on the 22^{nd}, the wind gradually eases.

The biggest difference between the two events is the location of the wind effects. Storm Angus had the strongest effects in the south of the UK, which has an impact on the measured transport starting in this area. It might have a smaller impact on the wind speeds in the study area, although the effects in the storm area are stronger than those of the even on the 6^{th}. During that event, the wind effects are more local, but less strong, causing a lower impact on the transport.

An increase in transport before and after the events is present. The reason for this could be that the low pressure systems have a cyclonic effect. The low pressure area is surrounded by higher pressures, which means that before the low pressure system arrives, the pressure first is higher. Then, when the low pressure system moves away, the pressure increases again. If this is combined with a turning of the wind direction back to the transport direction, the transport increases.

4.2.3 Propagation of signals

Feie-Shetland is also the only section with a lag from the Ellet Line, the lag being four days. However, this lag corresponds to a correlation of only 0.21. This would indicate that the lag might not be based entirely on signals with the same origin. The difference might also be caused by interference of the NCC.

The zero day lag would imply that the signals are all propagated within a day. As the correlation decreases with greater distance from the Ellet Line, this might suggest that most signals are indeed propagated within a day, and are therefore caused by meteorological circumstance. Signals originating from local changes in the Irish or Clyde Sea probably take longer to travel to the other sections.

4.2.4 T-S diagrams

The results from the T-S diagrams are as expected. Deeper water, further away from the coast, is found to be more saline and colder, shallower water, found near the coast is warmer and fresher. Also, the salinity throughout the months is quite stable, between 34.2 and 35.3. The temperature shows very clear seasonal heating, with the coldest water found in February and March, and the warmest water found just after summer, in September. The Wave Glider measurements are placed in the higher temperature range, and comply with the AMM7 points for September. The salinity in the North Minch is as expected low (<35.0), indicating transport here consists of the Scottish Coastal Current. This section does not extend as far out towards the shelf edge as the other sections, and transport consists mostly of water from the Scottish Coastal Current.

Usually in a T-S diagram, points on a straight line between two water masses would indicate that the water is a mixture of these water masses. In this case, some of the deeper points would be expected to consist of MNAW and NAW. However, MNAW is usually only found in the Faroe Shetland Channel. Another explanation for water found on this line could be that it originates from a branch of the North Atlantic Current further offshore in the North Atlantic Ocean (Dooley et al., 1976). This current has salinities between 35.30 and 35.40. The water at deeper points, and at the point further away from the coasts might originate from this current.

Finally, some differences are seen in the mean temperatures and salinities of the sections. The temperature seems to decrease from Shelf-4 (T = 10.51 °C) towards Shelf-2 (T = 10.18 °C). This might be the result of less local heating, as the AMM7 data in Figure 4.2 also shows that the water is colder further away from the Scottish mainland. This is also consistent with Holliday et al. (2015), who explain that the upper ocean is warmest, most saline and deepest in the Eastern Rockall Trough, and becomes colder, fresher and shallower when moving northwest. The North Minch also has a significant lower mean salinity, which is caused by the fact that the current here consists mostly of SCC water.

4.3 Limitations

The Wave Gliders studied in this research were only deployed for a short period of time (11 days), making it impossible to determine other tidal constituents than M2. Furthermore, the mis-timing of the MASSMO mission meant there were no moorings or other instruments deployed in the same time period in that area. Therefore, the Wave Glider data is limited and cannot easily be compared to measurements in the same circumstances. A longer deployment time would have increased the reliability of the Wave Glider data, and would have made more analyses possible. However, even with the short time period, the results already demonstrate the potential of these platforms.

Also, as the Wave Gliders followed the track only once, there was both spatial and temporal variability, with just one to three measurements for each location. This makes it difficult to determine whether the variations are caused by the spatial or temporal changes or both. Only Box 4 contained several days in a small spatial domain, and this box showed that a large amount of the variability is caused by the tides. This means that some of the noise is probably removed by decreasing the spatial variability.

Finally, little was known about the pre-processing of the Wave Glider data. The oxygen measurements could not be used because there was no information about the units or transformation of these measurements. Therefore, in the future, it would be useful to have good metadata about the pre-processing, or maybe on the programming of the Wave Glider track.

4.4 Implications

This research combined the use of Wave Gliders with the understanding of transport and circulation on the Scottish Continental Shelf. In previous research, transport and circulation on the shelf have already been studied. Transport through the Minch ((Hill et al., 1997);(McKay et al., 1986)), the Extended Ellet Line (Holliday et al., 2015), the FIC (Turrell et al., 1990);(Huthnance et al., 2009) and drivers of variability ((Huthnance, 1997);(Holt and Proctor, 2008)) have all been studied before. A lot about transport across the shelf, the variability in it, and drivers of this variability are already known. Sherwin et al. (2008) used ocean gliders to determine tidal fronts. Sea wave spectra are analysed using a Wave Glider by Alvarez (2015).

This study has combined Wave Gliders and investigating transport variability, and has shown that Wave Gliders can be very useful both in and outside research. In oceanographic research, Wave Gliders can be used for analyses of the tide, temperature, salinity, and transport across a section, as was shown by this study. Using different sensors, they would also be useful in other (research) fields.

Due to their relative small size and their ability to follow a pre-programmed course, even in tough weather circumstances, Wave Gliders could be very useful to access places ships cannot go. For example, Wave Gliders were used in the Great Barrier Reef to monitor the water conditions and water quality (Liquid Robotics Inc., 2020c). During this deployment, the Wave Gliders proved capable of staying on their course. That was also confirmed in this study, where all three Wave Gliders followed roughly the same path. Therefore, Wave Gliders would be very useful in monitoring coral reefs. However, coral reefs are not the only places that might be difficult to access. With the development of more and more wind parks at sea, Wave Gliders could also be used to monitor water quality or help determine the effect of these wind parks on marine life.

Also in more accessible areas, Wave Gliders could be a suitable replacement for traditional techniques. For example, in the Netherlands, one of the ferries between the island Texel and Den Helder is equipped with an ADCP (TESO, 2020). This ADCP measures the current velocities, which are then used to determine the amount of suspended sediment, and the topography of the seabed. These results are used to calculate the exchange of water and sediment between the North Sea and Wadden Sea. Furthermore, temperature and salinity sensors are also placed underneath the ferry, as well as light sensors to determine the amount of plankton. While the use of a ferry instead of a research vessel already saves time and money, it also limits the times and locations at which measurements can be taken. A Wave Glider could be used in between crossings, at night, or to cover a greater area.

As Wave Gliders are cost-effective and can be deployed for long periods of time, they could also be used to (partly) replace research ships. Water samples (Liquid Robotics Inc., 2020d) and other measurements usually collected by research ships, could also be taken by a Wave Glider. This would not only reduce the costs, but also allow more flexibility in when the measurements are taken. Furthermore, a Wave Glider could be used to upload data from other instruments, and then transmit it using its satellite connection. For example, seismic detection instruments are often placed on the seabed, at a depth of several kilometres. A Wave Glider could position itself above this, upload the data from the instrument, and then send it to the coast (Liquid Robotics Inc., 2020e). This allows for continuous monitoring of seismic activity, which is useful in predicting tsunamis, for example.

Chapter 5

Conclusions

The aim of this research was *to determine the applicability of Wave Gliders in observing and understanding oceanographic processes*. This aim was translated in the following research question:
"How can Wave Gliders be used to improve the understanding of oceanographic processes, using the Scottish Continental Shelf as a case study?"
To answer this main research question, three sub-questions were used to guide the research:

1. What is the quality of the data retrieved from the Wave Gliders during the MASSMO-3 mission, when compared to historical and modelled data?

2. What is the variability of the circulation on the Scottish Continental Shelf (SCS) in the region of the northern tip of the Western Isles?

3. How does the transport on the SCS and along its subsequent path into the North Sea vary?

5.1 SQ1: Data quality

What is the quality of the data retrieved from the Wave Gliders during the MASSMO-3 mission, when compared to historical and modelled data?

To determine the capability of the Wave Glider to capture tidal movements, statistical analyses (RMSE and correlation) and a tidal analysis were performed. From the results, it became clear that overall, the Wave Glider is capable of capturing the tides. The combination of spatial and temporal variation caused some issues, and a sharp turn in the track made data in that area unreliable. However, even with these issues, the Wave Glider data reproduced the M2 tide of the TMD with a RMSE of only 1-3 $cm\ s^{-1}$ (an error of 6-15%), and a correlation of 0.98-0.99. The tidal analysis proved that the Wave Glider is capable of estimating the tidal ellipses. It also showed that, when spatial variability was low, the percentage of variability explained by the tides was higher than if the entire track was taken into account. Therefore, it could be concluded that a long Wave Glider track, that covers a large area, could cause some extra noise in the time series.

5.2 SQ2: Circulation

What is the variability of the circulation on the Scottish Continental Shelf (SCS) in the region of the northern tip of the Western Isles?

To analyse the Wave Glider's ability to observe transport on the shelf, the transport across one of the sections on the Wave Glider track was calculated using the Wave Glider data and AMM7 data. Here, the Wave Glider gave a transport rate that was slightly lower than the AMM7 data, but was still well within the standard deviation of the AMM7 transport. Therefore, it can be concluded that a Wave Glider is useful in determining transport through sections. Next, transport across other sections was calculated, and an analysis of the temperature and salinity was performed. It appeared that there is an increase in transport between Shelf-3 and Shelf-2, this might be connected to an Atlantic Inflow between those two sections. Furthermore, the influence of two meteorological events in November 2016 was investigated. This showed that the transport is very depending on the wind direction and speed. This mostly had an effect on the Shelf sections, as these are more exposed than the North-Minch section. The T-S diagrams indicated that most of the shallower points, with smaller distance to the coast, carried water from the Scottish Coastal Current. The deeper and further off-shore points appeared to have some North Atlantic Water. The shelf seas are all quite shallow (<500 metres), which meant that seasonal heating also was clearly visible. The Wave Glider data here also seemed to be accurate.

5.3 SQ3: Transport on the main path of Atlantic Water from the shelf edge to the North Sea

How does the transport on the SCS and along its subsequent path into the North Sea vary

The third sub-question was answered by calculating the transport from the AMM7 data, and then investigating the propagation of the signals between the sections. First of all, the sections studied in this sub-question also showed an increase in transport somewhere between Shelf-4 and Shelf-0. The transport increases from the Ellet Line towards Shelf-0. Results from cross-correlations between each section and the Ellet Line indicated that the signals are propagated within one day, except for Feie-Shetland, where the lag was four days. If the signals are caused by meteorological events in the vicinity of all sections, this 0-day lag makes sense. The four-day lag might be caused by the interference of the Norwegian Coastal Current.

5.4 Overall conclusion

The answers on the sub-questions have shown that the Wave Glider is capable of capturing the tidal movements, and is useful in calculating transport across sections. Therefore, it can be concluded that Wave Gliders can be used to improve the understanding of oceanographic processes. However, there are some stipulations to this. First of all, a time period of 11 days is too short to capture any other tidal constituent than M2. Also, the short time series has an impact on the overall data quality. Furthermore, spatial variability should be kept to a minimum, especially sharp turns in the track. If these issues are taken into account, Wave Gliders can be useful by measuring current velocities, temperatures and salinity, and then using these parameters to determine tidal ellipses or calculate transport across a section and dividing this transport into water masses.

Chapter 6

Recommendations

In this chapter, some recommendations are made, both scientific and practical.

6.1 Scientific

1. **Determine the exact influence of spatial and temporal variability on the Wave Glider data**
   A longer deployment period would increase the opportunity to box results, by, for example, creating multiple smaller boxes. This would help to determine the impact of spatial variability even more. Furthermore, a simple track, such as a straight line, would help in determining the impact of temporal variability.

2. **Determine cause of variations in transport**
   Further research is needed to determine the exact cause of the increase in transport between Shelf-3 and -2.

   - One way to do this, would be by determining the temperature and salinity of the water masses through the sections. This was partly done during this research, however, it was not determined what the quantities of each water mass were. If this would be done, differences between the sections can be examined and the cause of the increase in transport might be determined. Also, a cross-section with temperature, salinity and velocity could help in determining the water masses.
   - Another way to determine the cause of the increase in transport would be to take some sections in between those two, to determine whether it is a gradual increase, or a sudden increase. These sections could be taken from a model, or investigated by Wave Gliders.

3. **Feie-Shetland**
   As multiple currents cross the Feie-Shetland section, the variations cannot be directly related to the variations in the other sections on the main path of Atlantic Water from the shelf edge into the North Sea. It might be worth it to split the section in at least two parts, where the midpoint is at the Norwegian Trench. Then, the Norwegian Coastal Current can be studied separated from the transport along the Main Transport Path.

4. **Oxygen measurements**
   In this study, there were oxygen measurements available. However, there was no metadata as to what the unit was, or what pre-processing was performed on these measurements. Therefore, it might be interesting to determine the quality of this parameter as well.

5. **Another model**
   This study only compared the Wave Glider to the TMD and AMM7 data. However, another model might be useful to determine how much of the uncertainty was caused by the models, and how much by the Wave Glider.

6.2 Practical

This research has shown that Wave Gliders can be very useful in understanding oceanographic processes, specifically calculating transport and determining tidal ellipses, temperatures and salinities. To ensure the Wave Glider is giving the most accurate results, some recommendations for the deployment strategy should be taken into account.

1. **Sharp turns**
   Sharp turns have a negative impact on the measurements, and should be avoided as much as possible. If it is not possible to avoid sharp turns, data measured in the hours before and after the turn might be unreliable.

2. **Longer deployment period**
   A longer deployment period would increase the data quality and would give the opportunity of analysing several tidal constituents, instead of just M2. As most areas experience a strong influence from both the M2 and S2 tidal constituent, these two should at least be analysed. Therefore, a minimum deployment period of 355 hours is recommended.

3. **Multiple Wave Gliders**
   During MASSMO-3, three Wave Gliders were deployed. Only one had an ADCP. One of the other Wave Gliders was at a different depth (20 metres instead of 8 metres). This made comparison between the three Wave Gliders difficult. It might be nice to have several Wave Gliders either deployed at the same time, which would make it easier to compare a single data point to other Wave Gliders, or as a staggered deployment, so each data point has measurements at different times. Also, Wave Gliders could be used at one single depth, so they can be compared easily. On the other hand, having Wave Gliders measure at different depths, would lead to more information on temperatures and salinities in the water column.
   One possible strategy would be to deploy Wave Gliders in multiple pairs, with one Wave Glider at one depth (e.g. 8 metres), and the other on another depth (e.g. 20 metres). Then, a second pair, with Wave Gliders at those same two depths, could leave a certain amount of time later, and follow the same path. This would also solve the interference of the sub with the ADCP.

4. **Additional sensors**
   In this study, Wave Gliders only measured current velocities, temperatures, salinities and oxygen. For future deployments, it might be useful to add other instruments, for example, a light sensor to chlorophyll-a. Also, in this study, the ADCP only measured until a depth of 25 metres, whereas the water depth was several hundred metres. It might be useful to have measurements that reach the seabed, so a better understanding of the entire water column can be reached.

5. **Metadata**
   The metadata of the Wave Gliders used in this study was scarce or non-existent. Therefore, some measurements could not be used (the oxygen measurements), while other

could not be fully placed into context. Therefore, metadata should always be complete, easily available, and kept in a logical place.

6. **Other data**
   To be able to compare the Wave Glider data with other measured data, it might be worth it to also deploy some oceanographic moorings in the vicinity of the Wave Glider track. This would give opportunity to analyse the data quality of the Wave Glider some more, but would also be helpful to provide context in case the Wave Glider fails to record data.

Bibliography

A. Alvarez. Assessment of sea wave spectra using a surfaced glider. *Deep Sea Research Part I: Oceanographic Research Papers*, 102:135–143, 8 2015. ISSN 09670637. doi: 10.1016/j.dsr.2015.04.015. URL `https://linkinghub.elsevier.com/retrieve/pii/S0967063715000898`.

J. M. Baxter, I. L. Boyd, M. Cox, A. E. Donald, S. J. Malcolm, H. Miles, B. Miller, and C. F. Moffat. *Scotland's Marine Atlas*. Marine Scotland, 2011.

B. Berx, B. Hansen, S. Østerhus, K. M. Larsen, T. Sherwin, and K. Jochumsen. Combining in situ measurements and altimetry to estimate volume, heat and salt transport variability through the faroe–shetland channel. *Ocean Science*, 9:639–654, 7 2013. ISSN 1812-0792. doi: 10.5194/os-9-639-2013. URL `https://www.ocean-sci.net/9/639/2013/`.

Copernicus. Atlantic-european north west shelf-ocean physics reanalysis, 2018. URL `https://cds.climate.copernicus.eu/cdsapp#!/dataset/reanalysis-era5-single-levels?tab=overview`.

S. de Vreeze. *Observing ocean currents on the Scottish Continental Shelf using autonomous technology - literature review*. Universiteit Twente, 2020.

H. Dooley, J. Martin, and R. Payne. Flow across the continental slope off northern scotland. *Deep Sea Research and Oceanographic Abstracts*, 23:875–880, 9 1976. ISSN 00117471. doi: 10.1016/0011-7471(76)90854-8. URL `https://linkinghub.elsevier.com/retrieve/pii/0011747176908548`.

G. D. Egbert and S. Y. Erofeeva. Efficient inverse modeling of barotropic ocean tides. *Journal of Atmospheric and Oceanic Technology*, 19:183–204, 2 2002. ISSN 0739-0572. doi: 10.1175/1520-0426(2002)019⟨0183:EIMOBO⟩2.0.CO;2. URL `http://journals.ametsoc.org/doi/abs/10.1175/1520-0426%282002%29019%3C0183%3AEIMOBO%3E2.0.CO%3B2`.

W. J. Emery and R. E. Thomson. *Data Analysis Methods in Physical Oceanography*. Elsevier, 2001. ISBN 9780444507563. doi: 10.1016/B978-0-444-50756-3.X5000-X. URL `https://linkinghub.elsevier.com/retrieve/pii/B9780444507563X5000X`.

L. Erofeeva and G. Egbert. European shelf, 2008, 2010. URL `http://people.oregonstate.edu/~erofeevs/ES.html`.

E.U. Copernicus Marine Service Information. Atlantic-european north west shelf-ocean physics reanalysis, 2018. URL `http://marine.copernicus.eu/services-portfolio/access-to-products/?option=com_csw&view=details&product_id=NORTHWESTSHELF_REANALYSIS_PHY_004_009`.

J. A. Graham, E. O'Dea, J. Holt, J. Polton, H. T. Hewitt, R. Furner, K. Guihou, A. Brereton, A. Arnold, S. Wakelin, J. M. C. Sanchez, and C. G. M. Adame. Amm15: a new high-resolution nemo configuration for operational simulation of the european north-west shelf.

Geoscientific Model Development, 11:681–696, 2018. doi: 10.5194/gmd-11-681-2018. URL https://www.geosci-model-dev.net/11/681/2018/.

B. Hansen and S. Østerhus. North atlantic–nordic seas exchanges. *Progress in Oceanography*, 45:109–208, 2 2000. ISSN 00796611. doi: 10.1016/S0079-6611(99)00052-X. URL https://linkinghub.elsevier.com/retrieve/pii/S007966119900052X.

A. E. Hill, K. J. Horsburgh, R. W. Garvine, P. A. Gillibrand, G. Slesser, W. R. Turrell, and R. D. Adams. Observations of a density-driven recirculation of the scottish coastal current in the minch. *Estuarine, Coastal and Shelf Science*, 45:473–484, 1997. ISSN 0272-7714. doi: https://doi.org/10.1006/ecss.1996.0198. URL http://www.sciencedirect.com/science/article/pii/S0272771496901985.

N. P. Holliday, S. A. Cunningham, C. Johnson, S. F. Gary, C. Griffiths, J. F. Read, and T. Sherwin. Multidecadal variability of potential temperature, salinity, and transport in the eastern subpolar north atlantic. *Journal of Geophysical Research: Oceans*, 120: 5945–5967, 9 2015. ISSN 2169-9275. doi: 10.1002/2015JC010762. URL https://onlinelibrary.wiley.com/doi/abs/10.1002/2015JC010762.

J. Holt and R. Proctor. The seasonal circulation and volume transport on the northwest european continental shelf: A fine-resolution model study. *Journal of Geophysical Research*, 113:C06021, 6 2008. ISSN 0148-0227. doi: 10.1029/2006JC004034. URL http://doi.wiley.com/10.1029/2006JC004034.

J. M. Huthnance. North sea interaction with the north atlantic ocean. *Deutsche Hydrographische Zeitschrift*, 49:153–162, 9 1997. ISSN 0012-0308. doi: 10.1007/BF02764030. URL http://link.springer.com/10.1007/BF02764030.

J. M. Huthnance, J. T. Holt, and S. L. Wakelin. Deep ocean exchange with west-european shelf seas. *Ocean Science*, 5:621–634, 2009. doi: 10.5194/os-5-621-2009. URL https://www.ocean-sci.net/5/621/2009/.

Igis Map. Bearing angle, 2020. URL https://www.igismap.com/map-tool/bearing-angle.

M. Inall, P. Gillibrand, C. Griffiths, N. MacDougal, and K. Blackwell. On the oceanographic variability of the north-west european shelf to the west of scotland. *Journal of Marine Systems*, 77:210–226, 5 2009. ISSN 09247963. doi: 10.1016/j.jmarsys.2007.12.012. URL https://linkinghub.elsevier.com/retrieve/pii/S0924796308002224.

S. Jones, F. Cottier, M. Inall, and C. Griffiths. Decadal variability on the northwest european continental shelf. *Progress in Oceanography*, 161:131–151, 2 2018. ISSN 00796611. doi: 10.1016/j.pocean.2018.01.012. URL https://linkinghub.elsevier.com/retrieve/pii/S0079661117302094.

Liquid Robotics Inc. Japan's first long-term ocean observation network, 2020a. URL https://www.liquid-robotics.com/customer-stories/japans-first-long-term-ocean-observation-network/.

Liquid Robotics Inc. Monitoring marine protected areas, 2020b. URL https://www.liquid-robotics.com/customer-stories/monitoring-marine-protected-areas/.

Liquid Robotics Inc. Wave glider missions with the australian institute of marine science, 2020c. URL https://www.liquid-robotics.com/customer-stories/wave-glider-missions-with-the-australian-institute-of-marine-science/.

Liquid Robotics Inc. On-demand water sampling, 2020d. URL https://www.liquid-robotics.com/customer-stories/on-demand-marine-water-sampling/.

Liquid Robotics Inc. Real-time, deep ocean seismic detection, 2020e. URL https://www.liquid-robotics.com/customer-stories/real-time-deep-ocean-seismic-detection/.

Maritime Robotics AS. Atlantic-european north west shelf-ocean physics reanalysis, 2019. URL https://www.maritimerobotics.com/wave-glider.

W. McKay, M. Baxter, D. Ellett, and D. Meldrum. Radiocaesium and circulation patterns west of scotland. *Journal of Environmental Radioactivity*, 4:205–232, 1986. ISSN 0265931X. doi: 10.1016/0265-931X(86)90011-1. URL https://linkinghub.elsevier.com/retrieve/pii/0265931X86900111.

National Oceanography Centre. Atlantic-european north west shelf-ocean physics reanalysis. URL https://noc.ac.uk/files/documents/business/POLPRED-HydroDLL.pdf.

National Oceanography Centre. Massmo 5, 2018. URL https://mars.noc.ac.uk/missions/massmo-5.

S. P. Neill, A. Vögler, A. J. Goward-Brown, S. Baston, M. J. Lewis, P. A. Gillibrand, S. Waldman, and D. K. Woolf. The wave and tidal resource of scotland. *Renewable Energy*, 114:3–17, 12 2017. ISSN 09601481. doi: 10.1016/j.renene.2017.03.027. URL https://linkinghub.elsevier.com/retrieve/pii/S0960148117302082.

R. A. Olson. Communications architecture of the liquid robotics wave glider. *IFAC Proceedings Volumes*, 45:255–259, 2012. ISSN 14746670. doi: 10.3182/20120410-3-PT-4028.00042. URL https://linkinghub.elsevier.com/retrieve/pii/S1474667016306115.

R. Pawlowicz, B. Beardsley, and S. Lentz. Classical tidal harmonic analysis including error estimates in matlab using t-tide. *Computers Geosciences*, 28:929–937, 10 2002. ISSN 00983004. doi: 10.1016/S0098-3004(02)00013-4. URL https://linkinghub.elsevier.com/retrieve/pii/S0098300402000134.

M. Porter, A. Dale, S. Jones, B. Siemering, and M. Inall. Cross-slope flow in the atlantic inflow current driven by the on-shelf deflection of a slope current. *Deep Sea Research Part I: Oceanographic Research Papers*, 140:173–185, 10 2018. ISSN 09670637. doi: 10.1016/j.dsr.2018.09.002. URL https://linkinghub.elsevier.com/retrieve/pii/S0967063718301560.

J.-Y. Reynaud and R. W. Dalrymple. *Shallow-Marine Tidal Deposits*. 2012. doi: 10.1007/978-94-007-0123-6_13. URL http://link.springer.com/10.1007/978-94-007-0123-6_13.

P. M. F. Sheehan, B. Berx, A. Gallego, R. A. Hall, K. J. Heywood, S. L. Hughes, and B. Y. Queste. Shelf sea tidal currents and mixing fronts determined from ocean glider observations. *Ocean Science*, 14:225–236, 3 2018. ISSN 1812-0792. doi: 10.5194/os-14-225-2018. URL https://www.ocean-sci.net/14/225/2018/.

T. J. Sherwin, S. L. Hughes, W. R. Turrell, B. Hansen, and S. Østerhus. Wind-driven monthly variations in transport and the flow field in the faroe–shetland channel. *Polar Research*, 27:7–22, 1 2008. ISSN 1751-8369. doi: 10.1111/j.1751-8369.2007.00036.x. URL https://polarresearch.net/index.php/polar/article/view/2860.

TESO. Teso en duurzaamheid, 2020. URL https://www.teso.nl/over-teso/teso-en-duurzaamheid/.

L. Thompson, S. Hautala, and K. Kelly. *Local character of tides*. 2005.

M. Tonani. *Project User Manual for North-West Shelf Physical Reanalysis Products NORTHWESTSHELF_REANALYSIS_PHY_004_009*. EU Copernicus Marine Service, 2019.

W. R. Turrell, E. W. Henderson, and G. Slesser. Residual transport within the fair isle current observed during the autumn circulation experiment (ace). *Continental Shelf Research*, 10:521–543, 1990.

UK Met Office. Dws_2016_11, 12 2016. URL https://digital.nmla.metoffice.gov.uk/IO_7396b355-b1df-4cbc-a0d3-0a1853082f29/.

L. Wang, Y. Li, Y. Liao, K. Pan, and W. Zhang. Dynamics modeling of an unmanned wave glider with flexible umbilical. *Ocean Engineering*, 180:267–278, 5 2019a. ISSN 00298018. doi: 10.1016/j.oceaneng.2019.03.047. URL https://linkinghub.elsevier.com/retrieve/pii/S0029801818311880.

P. Wang, X. Tian, W. Lu, Z. Hu, and Y. Luo. Dynamic modeling and simulations of the wave glider. *Applied Mathematical Modelling*, 66:77–96, 2 2019b. ISSN 0307904X. doi: 10.1016/j.apm.2018.08.027. URL https://linkinghub.elsevier.com/retrieve/pii/S0307904X18304293.

E. Williams. Latitude/longitude distance calculator, 2020. URL https://www.nhc.noaa.gov/gccalc.shtml.

R. Wynn. Massmo. *FOCUS*, pages 6–7, 2019.

Appendices

Appendix A

Bin 7

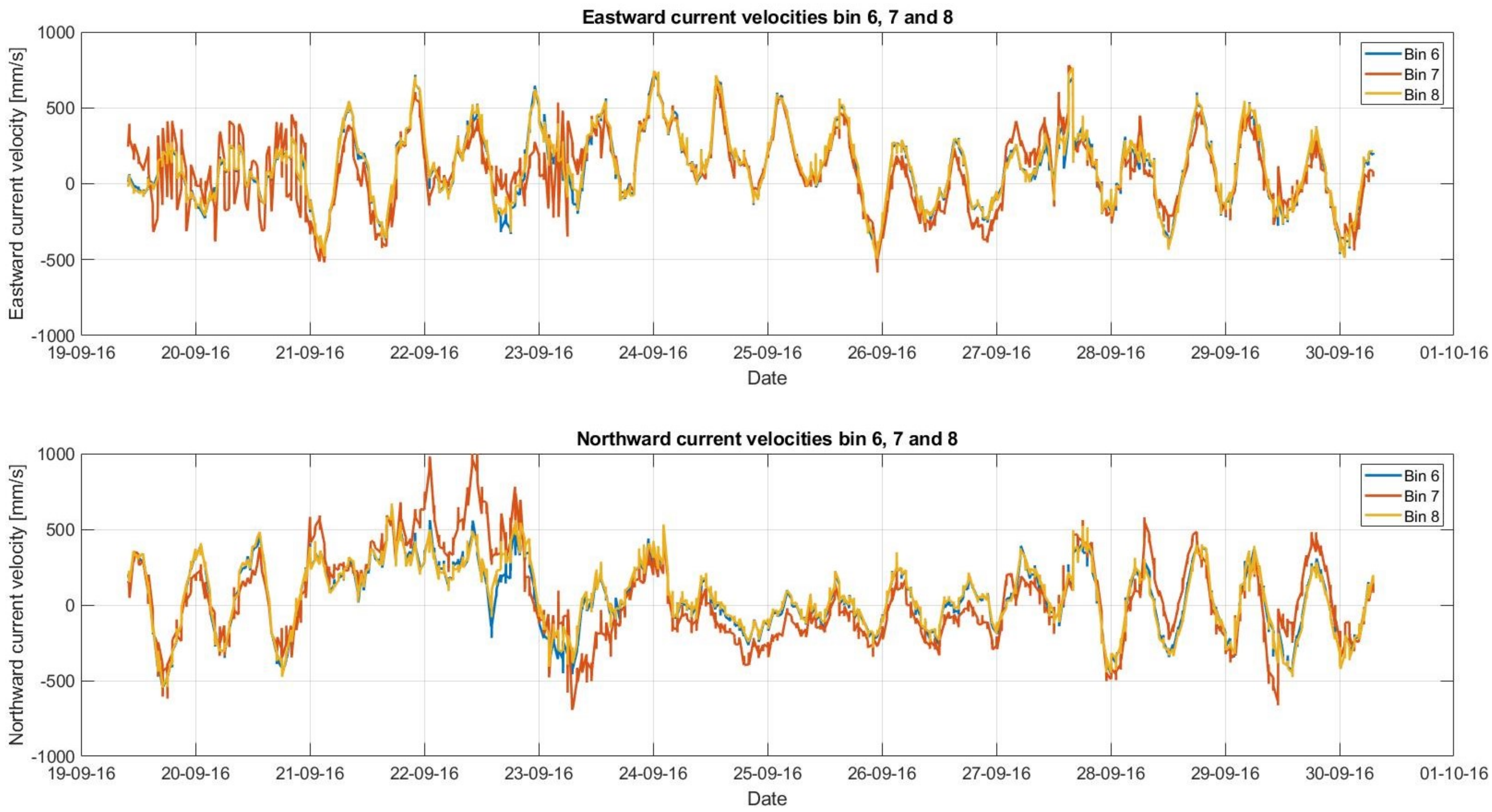

Figure A.1: Current velocities ($mm\ s^{-1}$) bin 6, 7 and 8 for the entire duration of the Wave Glider deployment, determined by the Wave Glider.

Appendix B

Predicted tides

B.1 Wave Glider

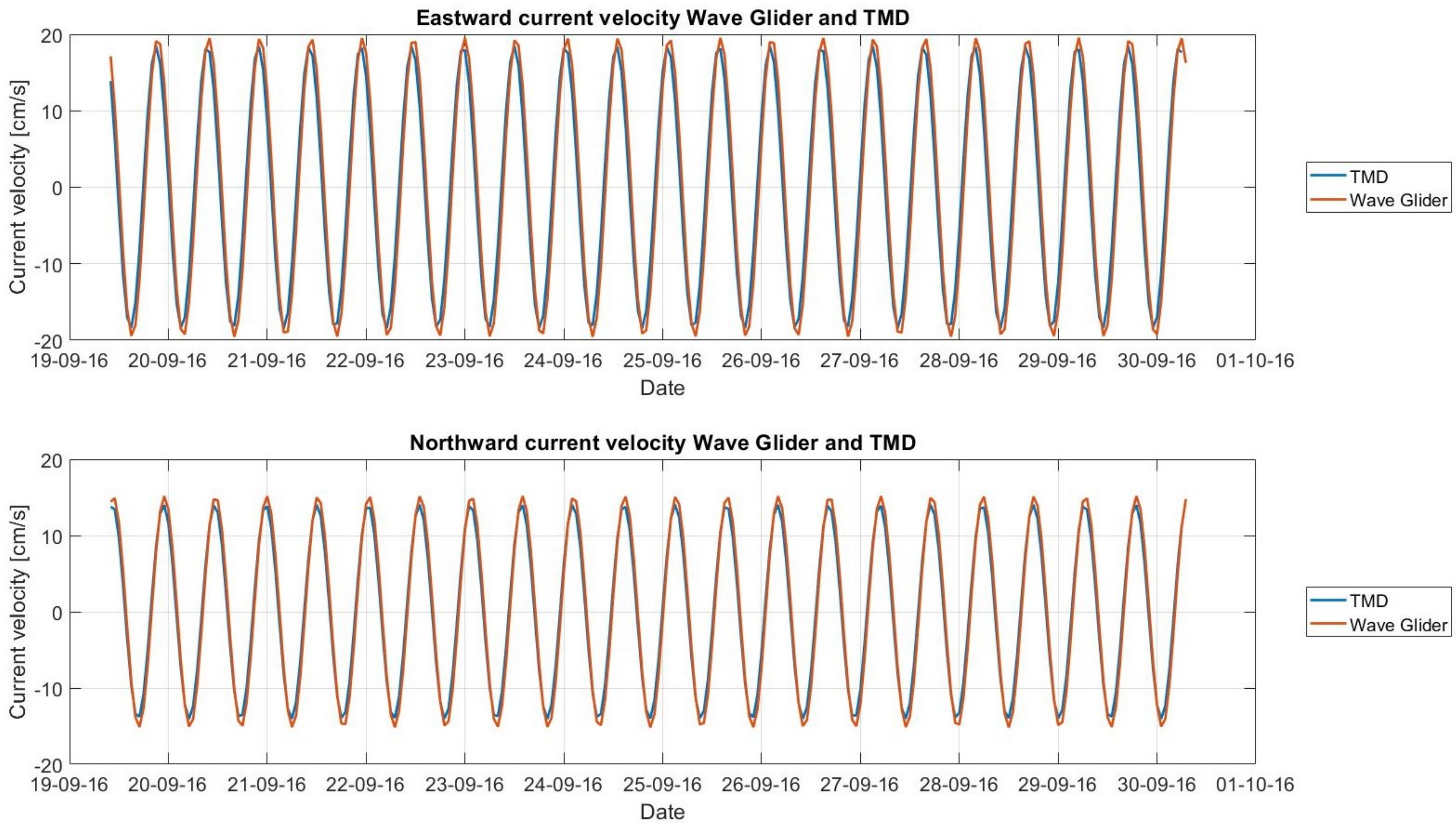

Figure B.1: Predicted tides $cm\ s^{-1}$ Wave Glider and TMD data, by t_tide.

B.2 Mooring

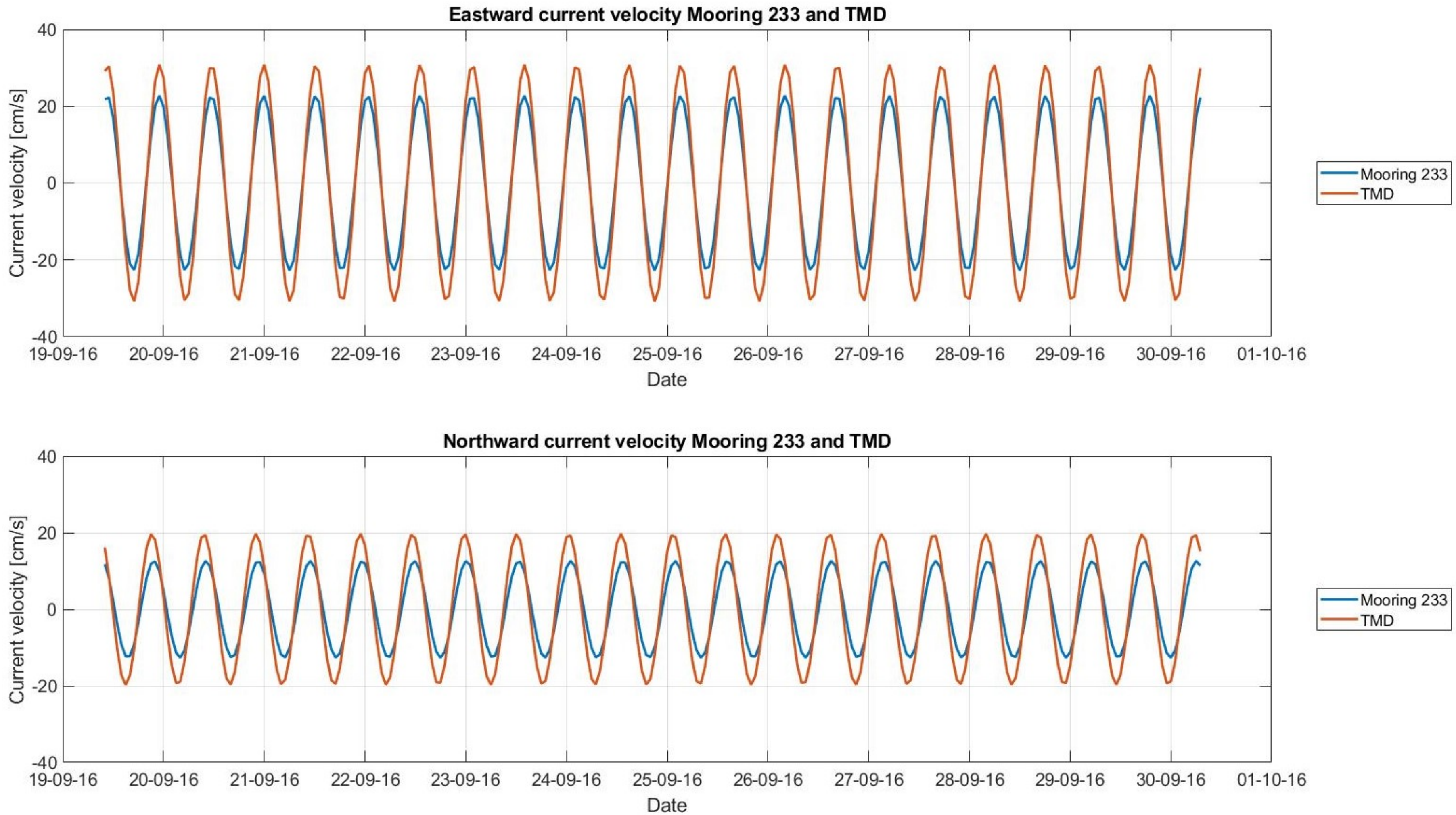

Figure B.2: Predicted tides $cm\ s^{-1}$ mooring CM233 and TMD at location 233, by t_tide.

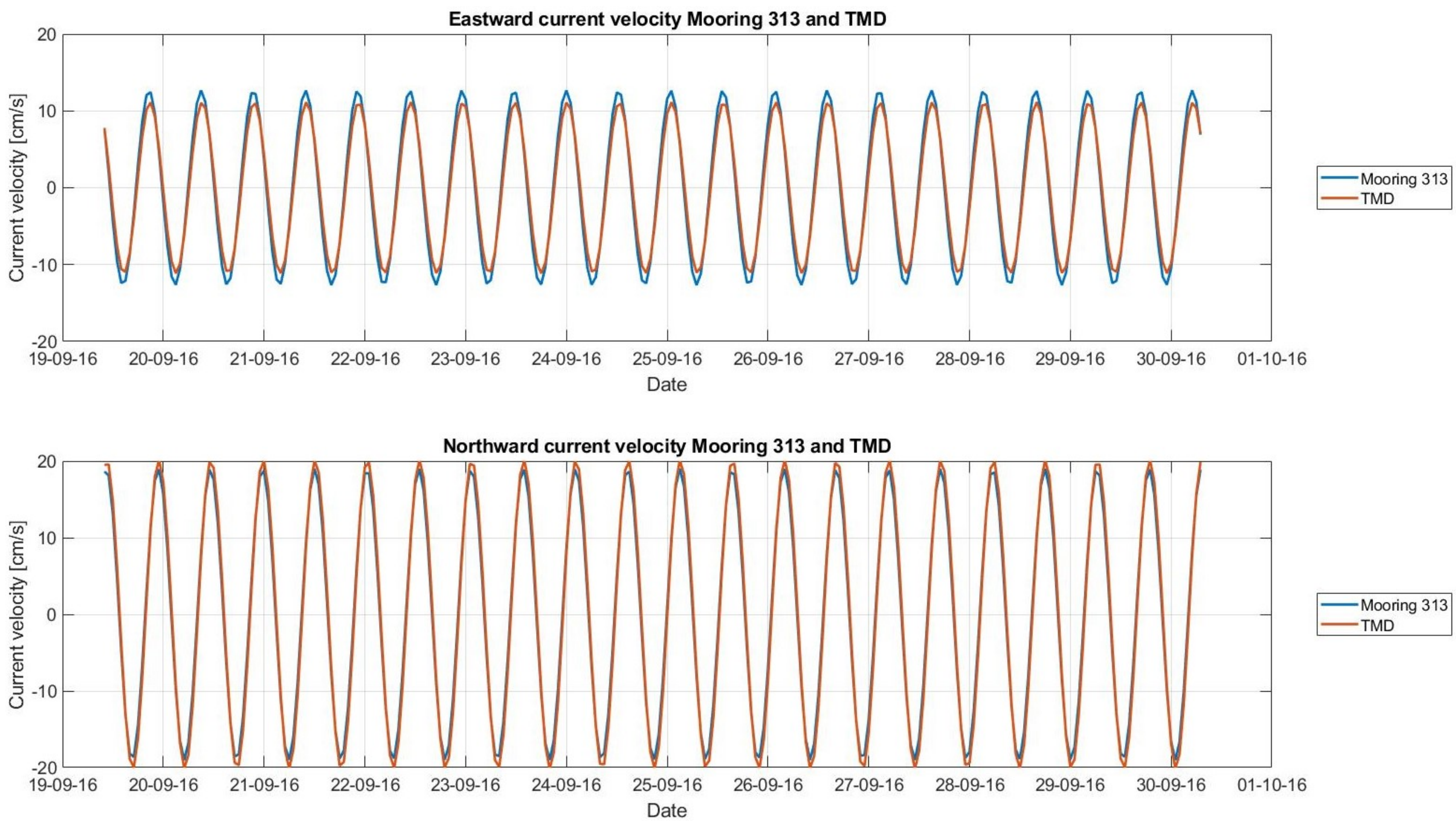

Figure B.3: Predicted tides $cm\ s^{-1}$ mooring CM313 and TMD at location 313, by t_tide.

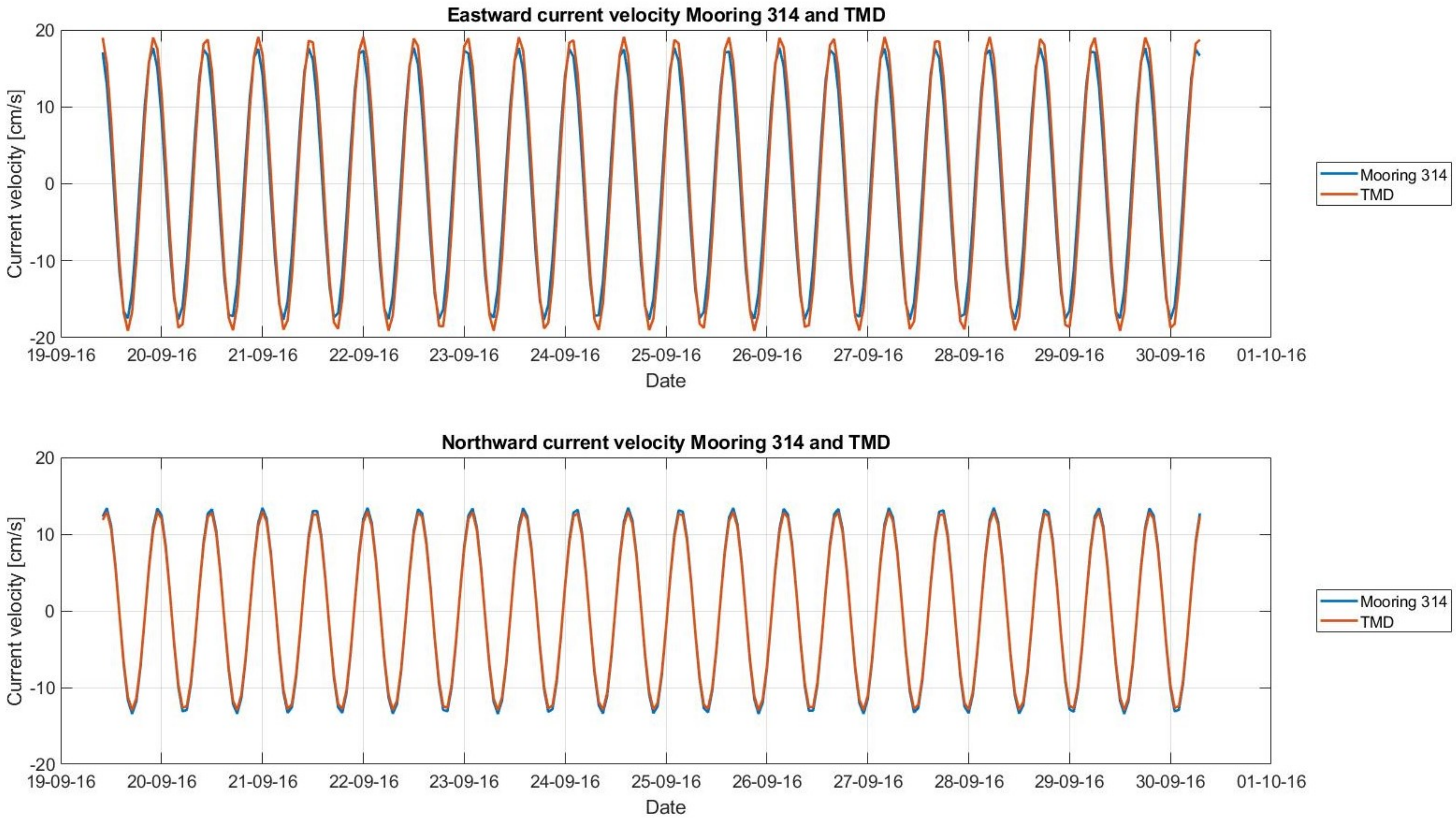

Figure B.4: Predicted tides $cm\ s^{-1}$ mooring CM314 and TMD at location 314, by t_tide.